

ALGERIAN REPUBLIC MINISTRY OF HIGHER EDUCATION
AND SCIENTIFIC RESEARCH

Order Number: /2024

Kasdi Merbah-Ouargla University

Faculty of Hydrocarbons, Renewable Energy and Earth and Universe Science

Department of Hydrocarbon Production

Master dissertation

Presented by

BELAHLOU Narimene – ZAHAF Maamar

To obtain Master's degree

Sector: Hydrocarbons

Option : Professional Production

- THEME -

**Experimental investigation of the influence
of pore geometry on laboratory water-oil relative
permeability and oil recovery**

Publicly supported on: 26 / 06 /2024

In front of the Jury

President	MILOUDI Mustapha	MAA	UKMO
Examiner	TOUAHRIA Abdeldjebar	MCB	UKMO
Supervisor	BOUFADES Djamila	MCA	UKMO
Co-supervisor	ADJOU Zakaria	Ph. D	UKMO

Academic year: 2023/2024

Acknowledgments

This research work was carried out at the Faculty of Hydrocarbons, Renewable Energies and Earth & Universe Sciences, Kasdi Merbah-Ouargla University.

*First of all, we would like to thank our thesis sponsor **Dr. ZAKARIA Adjou** and **Dr. DJAMILA Boufades** for having kindly helped and supported us throughout the realization of this work. We are also grateful for the confidence they have shown in us, which has enabled us to carry out this work successfully and independently.*

*My sincere thanks go to **Mr. MUSTAPHA Miloudi**, professor at Kasdi Merbah - Ouargla University, **Mr. ABDELJABAR Touahria**, professor at Kasdi Merbah - Ouargla University, for their participation in this jury as chairwoman and examiner. Their presence guarantees us a rigorous examination and a fair critique of our work.*

We would also like to thank our professors in the Department of Hydrocarbon Production. for their moral support throughout our academic career.

We would like also to thank our parents, brothers and sisters, who have shown us their trust and total support throughout our studies.

We would also like to thank all the people that we have omitted to mention and who have participated from near or far in the completion of this work.

Dedications

At the end of this journey, I would like to dedicate this humble work to those who have always been the light and support in my life, even in the darkest nights, my mom and dad.

To my dear siblings Sara, Anouar, Badreeddine, Intissar and Arwa whose accompanied me and shared with me the moments of joy, fun and sadness in life, I am very lucky to have you. I also thank my dear uncle for his support in choosing this vital specialisation.

To all the friends who have been like unborn brothers to me, each one by name, childhood friends, study friends, residential friends, thank you from the heart for everything.

To my honourable professor who taught me during all my academic years from primary to university and was the reason for my reaching this level.

To the man who always stood firm and who was the biggest brother I ever had and who accompanied me during these five years in good times and bad, I will never forget you, Dr. ADJOU Zakaria.

To all the laboratory Workers who were by our side during the preparation of the memorandum, especially Mrs. Hadjer, Latifa, Zahra and Hadja.

To my colleague Narimene Belahlou, who shared with me all the moments of this journey and who was very diligent and persistent, I thank God for having an exceptional person like you and I wish you success in this life.

To all the laboratory colleagues.

To my ambitious self who never gave up until the end.

MAAMAR Zahaf

Dedications

To my beloved parents, this work is dedicated to you. To my father for his endless support, encouragement, and desire to see me excel and develop. Your belief and trust in me have driven me to overcome challenges. To my mother, who is the true embodiment of resilience and devotion, your constant prayers have paved the way to each accomplishment, for your sacrifices, giving up so much of yourself to ensure that we, your children, could reach our highest potential. You have always pushed me for excellence.

To my precious siblings, Bouchra, Nadjib, and Adem, thank you for being there for me, for celebrating my successes. Your presence in my life has been a constant reminder of the importance of family and the role you each play in shaping me into the person i am today.

And I am honored to have you both by my side, especially during these five years away from you. Your trust and total support mean the world to me.

To my brother-in-law Zakaria. We are truly blessed to have you among us, thank you for your enormous support, your presence has always been a positive influence to me. I also dedicate this work the most precious gift You and my sister have brought into my life, my precious nephew, Aouab who has filled my life with indescribable happiness, and I pray for his protection and well-being always.

To the best roommate ever, Ikrem, more than a friend, you have been like a sister, providing spiritual and moral support throughout this journey. Thank you for being there for me every step of the way.

To my colleague Maamar Zahaf, sharing this journey with you has been invaluable. Your hard work, and camaraderie have made the process of this thesis both manageable and enjoyable.

My gratitude also goes to my esteemed supervisor, Dr. Adjou Zakaria. For your guidance and mentorship. You have been more than just a supervisor; you have been a trusted advisor and friend. Thank you for your commitment and for being a constant source of comfort and inspiration. Sir, it has been a wonderful honor working with you.

To myself, for never giving up, for pushing through the challenges, and for finally reaching this moment.

BELAHLOU Narimene

Abstract

Abstract

Pore geometry dictates the preferential pathways of fluids in the porous medium, impacting water-oil relative permeability and oil recovery efficiency.

This work investigates the

influence of pore geometry on laboratory-measured porosity, relative permeability and oil recovery on both three varied size homogeneous and heterogeneous samples based on sand and sand with 20% of clay, then a new PVC-designed mesofluidic system to visualize fluid-fluid displacement, to determine oil recovery and set up a preliminary investigation of thermal Enhanced Oil Recovery (TEOR). All the experiments were conducted under laboratory conditions. The results showed variations in oil relative permeability which increases as grain size increasing (0.643D for 500 μm , 0.535D for 250 μm , 0.503D for 125 μm and 0.654D for the polymodal sample). Also due to the presence of clay the polymodal sample revealed a decrease of oil relative permeability from 0.654D to 0.510D. The incremental oil recovered for the polymodal sample was 13 ml. For the PVC-designed mesofluidic system several fluid pathways were observed with 17.084 ml of oil recovery, where the steam was injected under 130 °C to extract an amount of 6% from 55.22% of the trapped oil.

Key words: Porous media, pore geometry, preferential pathway, relative permeability, PVC-designed mesofluidic system, steam injection.

Résumé

La géométrie des pores décrit les chemins préférentiels des fluides dans le milieu poreux, affectant la perméabilité relative d'eau et d'huile et l'efficacité de récupération d'huile. Ce travail étudie l'influence de la géométrie des pores sur la porosité, la perméabilité relative et la récupération de l'huile mesurées en laboratoire sur trois échantillons homogènes et hétérogène de différente dimension formé du sable et de la sable avec 20% d'argile, puis un nouveau système mesofluidique conçu par de PVC pour visualiser le déplacement fluide-fluide, et déterminer le recouvrement de l'huile et mettre en place une investigation préliminaire sur la récupération tertiaire d'huile par voie thermique (TEOR). Toutes les expériences ont été menées dans les conditions de laboratoire. Les résultats ont montré des variations de la perméabilité relative de l'huile qui augmente avec l'augmentation de la dimension des grains (0,643D pour 500 μm , 0,535D pour 250 μm , 0,503D de 125 μm et 0,654D pour l'échantillon polymodal). En raison de la présence d'argile, l'échantillon polymodal a révélé une diminution de la perméabilité relative d'huile de 0.654D à 0.510D. L'huile incrémentale récupérée pour l'échantillon polymodal était de 13 ml. Pour le système mesofluidique, plusieurs chemins de fluide ont été observés avec 17.084 ml de récupération d'huile, où la vapeur a été injectée sous 130°C pour extraire une quantité de 6% de 55,22% de l'huile piégée.

Mots clés : Milieux poreux, géométrie des pores, chemin préférentiel, perméabilité relative, système mesofluidique, injection de vapeur.

ملخص

تحدد هندسة المسام المسارات التفضيلية للسوائل في الوسط المسامي، مما يؤثر على الزنادية النسبية للماء و النفط وكفاءة استخلاصه. يُدرس هذا العمل تأثير هندسة المسام على المسامية والزنادية النسبية واستخلاص النفط المقاسة في المخبر على ثلاث عينات متجانسة وأخرى غير متجانسة ذات أبعاد مختلفة من الرمل ورمل مع 20% من الطين، ثم تصمم نظام موانع متوسطة جديد بواسطة PVC لنمذجة حركة السوائل، وتحديد عملية استخلاص النفط وإجراء تجزيق أولي بشأن الاستخلاص الحراري المعزز للنفط (TEOR). أجريت جميع التجارب تحت ظروف المخبر. حيث أظهرت النتائج اختلافات في الزنادية النسبية للنفط والتي تزداد مع زيادة حجم الحبيبات (0.643D لـ 500 ميكرومتر، 0.535 D لـ 250 ميكرومتر، 0.503 D لـ 125 ميكرومتر و D 0.654 للعينة من عدة الأبعاد). بسبب وجود الطين، كشفت العينة من عدة الأبعاد عن انخفاض في زنادية النفط النسبية من D0.654 إلى D0.510. كان النفط الإضافي المسنرد للعينة من عدة الأبعاد 13 مل. بالنسبة لنظام الموانع المتوسطة، تمت اللحظة مسارات من عدة للسوائل مع 17.084 مل من استخلاص النفط، حيث تم حزن البخار تحت درجة حرارة 130 درجة مئوية السخراج كفاءة 6% من 55.22% من النفط المحنن.

الكلمات المفتاحية: الوسائط المسامية، هندسة المسام، المسار التفضيلي، الزنادية النسبية، نظام الموانع المتوسطة، حزن البخار.

Table of content

Acknowledgements	I
Dedications	
Abstract	IV
Table of contents	VI
List of figures	IX
List of tables	XI
List of abbreviations	XII
General introduction	01
Chapter I: Porous medium fundamentals	
Introduction	03
I-1 Porous Medium	03
I-2- Porous Medium types	04
I-2-1 Unconsolidated porous media	04
I-2-2 Consolidated porous media	04
I-2-3 Homogeneous porous media	04
I-2-4 Isotropic and anisotropic media	04
I-3 Porous medium study scales	04
I-3-1 Molecule Scale	04
I-3-2 Particle Scale	05
I-3-3 Subsystem Scale	05
	II

I-4 Multiphase flow in porous media	06
I-4-1 Types of multiphase flow	06
I-4-2 Multiphase flow in isotropic porous media	07
I-4-3 Multiphase flow in anisotropic porous media	08
I-5 Static petrophysical properties	09
I-5-1 Porosity	09
I-5-2 Tortuosity.	12
I-5-3 Saturation	13
I-5-4 Interfacial tension	15
I-5-5 Capillary pressure	16
I-5-6 Wettability	17
Conclusion	19

Chapter II: Preferential flow pathways and oil recovery strategies

Introduction	20
II-1-Permeability	20
II-1-1 Absolute permeability	20
II-1-2 Effective permeability	21
II-1-3 Relative permeability	22
II-1-4 Permeability Classification according to the origin and formation process	22
II-1-5 Factors affecting permeability	22
II-1-6 Permeability measurements	24
II-1-7 Effect of wettability on relative permeability	26
II-1-8 Effect of capillary number on relative permeability	28
II-2 Preferential flow paths	29
II-3 Oil recovery	29
II-3-1-Primary recovery	29
II-3-2-Secondary recovery	30
II-3-3-Tertiary Recovery	32
II-4 Relationship between oil recovery and pore geometry	34
II-4-1 Pores size	34
II-4-2 Pores shape	34
II-4-3 Pores connectivity	34
II-4-4-Pores tortuosity	35
II-4-5-Pore Size Distribution	35
II-4-6-Heterogeneity	35
II-5 Pore-Scale phenomena in fluid flow	35
II-5-1 Snap-Off phenomenon	35
II-5-2 Jamin effect phenomena	36
II-5-3 Bypass phenomena	37
II-5-4 Water block phenomena	37
Conclusion	38
Conclusion and recommendations	82
Bibliographic references	85
Appendix	

List of figures

Figure I.1: Examples of porous media ($10 \times$ magnified): (A) beach sand, (B) sandstone; (C) limestone; Dry (D) rye bread; (E) wood; (F) human lung	03
Figure I.2: Different porous medium scales.	06
Figure I.3: Multiphase flow types.	07
Figure I.4: Schematic diagram of an isotropic porous medium where dark shapes are solids (rocks). (a) An idealized reservoir, and (b) Representative elementary volume (REV)	08
Figure I.5: Anisotropic rock physics modeling flow chart of a fractured tight sandstone reservoir	09
Figure I.6: Porosity in sandstones, a) ME image of the resin-filled pore network of a Fontainebleau sandstone with 4% porosity after acid dissolution of the grains b) Porosity model in sandstone from Bernabé (1991)	10
Figure I.7: a) porosity diagram in sandstone and b) porous network model (tubes and nodal pores)	10
Figure I.8: Different types of pores.	11
Figure I.9: Schematic Shape of pore and Pore Throat	12
Figure I.10: Diagram of tortuosity	13
Figure I.11: Intermolecular Forces as They Effect Interfacial Tension	16
Figure I.12: Rise of liquid in a capillary tube	17
Figure I.13: Wetting Angles for Various Wetting Properties	18
Figure I.14: Types of wettability in porous media: a) Free water wettability, b) Fractional wettability, c) Free oil wettability	19
Figure II.1: Effects of grains shape and size on permeability: A. Large, Flat Grains, B. Large, Rounded Grains, C. Very Small Irregular Grains	23
Figure II.2: Effects of clay on permeability: a. Sand grains without clay, b. Sand grains with clay	24
Figure II.3: Schematic illustration of an unsteady state relative permeability determination method	25

Figure II.4: Schematic illustration of a steady state relative permeability determination method	26
Figure II.5: schematic representation of the relative permeability curve	27
Figure II.6: Typical relative permeability curves of an oil-water pair for an oil-wettable system	27
Figure II.7: Typical curves for the relative permeability of an oil-water pair for a water-wettable system	28
Figure I.8: Conceptual drawing of three types of preferential flow	29
Figure II.10: Illustrating waterflooding technique of secondary recovery	30
Figure II.11: Recovery process and mechanism of SAGD	
Figure II.12: Snap-off diagram in a pore groove: The solid is black, the water is grey and the gas is white	
Figure II.13: Trapped capillary drop: Jamin effect	
Figure II.14: Bypassing phenomena illustration, a) Drainage Process, No Trapping, b) Drainage Process, Bypassing in Smaller Throat, c) Imbibition Process, Bypassing in Larger Throat	
Figure II.9: Primary recovery	

List of tables

Table I.1: Different porous medium scales	05
Table I.2: Rock wettability profiles according to the contact angle	18
Table II.1: Permeability range classification	21

List of abbreviations

PVC	Polyvinyl chloride
EOR	Enhanced oil recovery
SEM	Scanning Electron Microscopy
EDX	Energy Dispersive X-ray Spectroscopy
REV	Representative Elemental Volume
α	Phase
u_α	phase velocities (m/s)
Φ	Porosity of the porous medium (%)
ρ_α	Density of phase α (kg/m ³)
S_α	Saturation of phase α (%)
u_α	Velocity of phase (m/s)
q_α	Source/sink term for phase α (kg/m ³ ·s)
$k_{r\alpha}$	Relative permeability of phase α (D)
μ_α	Dynamic viscosity of α (cP)
K	Intrinsic permeability of the porous media (D)
p_α	Pressure of phase α (Pa)
g	Gravitational acceleration (m/s ²)
V_s	Volume of the solid (cm ³)
V	Total volume of rock (cm ³)
ρ	Density of the liquid (kg/m ³)

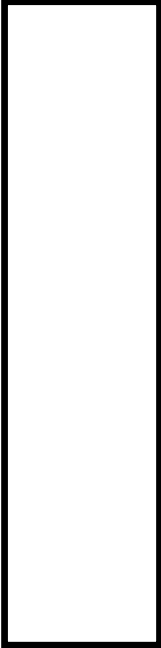
V_p	Pore space volume cm^3
ϕ_T	Total porosity (%)
ϕ_E	Effective porosity (%)
T	Tortuosity
L'	Length of a current line separating two points (m)
L	Distance between two points (m)
F	Formation factor (m)
D	Stands for the grain size
K	Permeability (D)
A	Constant
C	Kozeny-carman constant
V_o	Volume of oil (m^3)
V_w	Volume of water (m^3)
V_g	Volume of gas (m^3)
S_w	Water saturation (%)
S_o	Oil saturation (%)
S_g	Gas saturation (%)
S_{hc}	Hydrocarbon saturation (%)

S_{wi}	Irreducible water saturation (%)
COS	Critical oil saturation (%)
S_{or}	Residual oil saturation (%)
$A\alpha\beta$	Contact area (m ²)
β	Phase
ΔG	Gibbs free energy (Joule)
T	Temperature (°C)
P	Pressure (pa)
n	Number of moles (mol)
P_c	Capillary pressure (Pa)
σ_{12}	Interfacial tension between the two fluids (N/m)
θ	Contact angle between the fluid-fluid interface and the solid surface (pore wall) (°)
r	Radius of the pore throat (m)
σ_{ow}	Oil/water interfacial tension (N/m)
σ_{os}	Oil/solid interfacial tension (N/m)
σ_{ws}	Water/solid interfacial tension (N/m)
Q	Flow (cm ³ /s)
k	Permeability of porous rock (Darcy)

A	Cross-sectional area of rock (cm^2)
μ	Fluid viscosity (cP)
L	Length of rock sample (cm)
ΔP	Differential pressure (atm)
k_a	Absolute permeability (D)
k_{effo}	Oil effective permeability (mD)
k_{effg}	Gas effective permeability (mD)
k_{effw}	Water effective permeability (mD)
k_r	Relative permeability
i	Fluid phase oil, water or gas
L	Sample length (m)
K_{ro}	Oil relative permeability
K_{rw}	Water relative permeability
Ca	Capillary number

η	Viscosity of the displacing fluid (Cp)
v	Fluid velocity (m/s)
σ	Interfacial tension between water and oil N/m
IFT	Interfacial tension (N/m)
N_p	Cumulative oil production (m ³)
<i>OOIP</i>	Original oil in place (m ³)
R_{fw}	Formation water produced (m ³)
<i>RF</i>	Recovery factor %
<i>RFEOR</i>	Recovery factor achieved with EOR
<i>RF secondary</i>	Recovery factor achieved with secondary recovery methods.
Q	Heat energy transferred (Joule)
q_o	Oil production rate (m ³ /s)
V_b	Bulk volume of the reservoir (m ³)
<i>MR</i>	Volumetric heat capacity of the reservoir (J/m ³ ·K)
ΔT	Temperature difference between the injected steam and the reservoir (°C)
ϕ	Porosity of the reservoir (%)
dVs	Rate of change of the steam swept volume (m ³ /s)
<i>Soi</i>	Initial oil saturation (%)
<i>Boi</i>	Initial oil formation volume factor (m ³ /m ³)
<i>Sors</i>	Residual oil saturation after steam drive (%)
<i>Bos</i>	Oil formation volume factor after steam drive (m ³ /m ³)
<i>SAGD</i>	Steam-assisted gravity drainage
I_w	Water wetting index

V_{sw}	Volume of water spontaneously imbibed (m^3)
V_{fw}	Total volume of water imbibed (spontaneous + forced) (m^3)
I_o	Oil wetting index
V_{so}	Volume of oil spontaneously imbibed (m^3)
V_{fo}	Total volume of oil imbibed (spontaneous + forced). (m^3)
WI	wettability index
V_{or}	Residual oil volume (m^3)
V_r	Recovered oil volume (m^3)
m_{sat}	Mass of the sample totally saturated with brine (g)
m_{dry}	Mass of the dry sample (g)
A	Fluid passage section (cm^2)
μ	Fluid viscosity (cP)
dP	Pressure difference (atm)
dx	Length of the sample (cm)
Q_o	Volumetric flow rate of oil (cm^3/s)
Q_w	Volumetric flow rate of brine (cm^3/s)
μ_o	Oil viscosity (cP)
μ_w	Water viscosity (cP)
ΔP_o	Differential pressures of oil (atm)
ΔP_w	Differential pressures of water (atm)
K_{ao}	Oil absolute permeability (D)
K_{aw}	Water absolute permeability (D)



General Introduction

General introduction

Previous studies have demonstrated that the lithologic features of rocks impact their reservoir properties such as permeability, porosity, irreducible water saturation, and surface area. Due to this number of variations, one specific rock feature has the same magnitude of influence on different reservoir rock types. This relationship suggests that trying to define a reservoir solely based on readily accessible variables, such permeability or grain shape, carries some risk. With factors such as sorting, cementation can obscure their significance. Accurate fluid flow predictions depend on a geological understanding of the reservoir rock types and the ability to identify changes within them [01], [02].

Hypotheses

The study is based on several key hypotheses:

- The geometry and size distribution of pores within a porous medium significantly influence fluid flow dynamics and oil recovery efficiency with being increased as the grain size increases.
- Thermal enhanced oil recovery methods, particularly steam injection, improve oil mobility and recovery efficiency by reducing oil viscosity and altering fluid interactions within the pore spaces.
- Mesofluidic systems can accurately simulate the behaviour of multiphase flow in real reservoir conditions, providing valuable insights into fluid dynamics and displacement patterns; and variations in wettability and saturation levels within porous media critically affect the displacement efficiency of oil by injected water or steam [03],[04],[05],[06].

Problematic of the study

The primary problematic addressed in this work is how the heterogeneity in pore size distribution and connectivity, influenced by factors such as clay content impacts fluid-fluid displacement, and hydrocarbon recovery rates in porous media. Additionally, it explores whether thermal recovery methods can effectively mitigate these challenges to enhance overall recovery efficiency, as understood through real-time visualization and advanced experimental simulation techniques.

Objectives of the study

The key aims are to characterize the petrophysical features of diverse porous media, analyze the dynamics of two-phase water-oil flow, and evaluate the efficacy of thermal EOR

General introduction

methodologies, using mesofluidic models to simulate and visualize multiphase flow, and devising strategies for optimizing oil recovery based on these findings.

Organization of the dissertation

The manuscript is organised as follows:

The first chapter examines the essential properties of porous media, including porosity and permeability, which influence fluid storage and flow. It discusses wettability, capillary forces, dynamic flow phenomena, and multiphase flow dynamics, emphasizing the significance of petrophysical properties like porosity and saturation. The chapter also offers historical and theoretical insights, such as Darcy's Law, to provide a thorough understanding of fluid flow within porous materials.

The second chapter explores the enhancement of oil recovery by understanding and manipulating reservoir flow pathways. It addresses permeability and the formation of preferential flow paths, bypass, and water block phenomena. The chapter reviews enhanced oil recovery (EOR) methods like thermal recovery and chemical flooding, and discusses experimental and modelling techniques to optimize fluid flow and recovery strategies in porous media.



Chapter I

Porous media fundamentals

Introduction

Comprehending the phenomena occurring within porous medium across various scales is essential for understanding and optimizing processes of oil recovery. This chapter is grounded in the fundamental concepts surrounding porous media, its scales, identification, and characterization, from microscopic pore networks to macroscopic behaviors, we explore the diverse methodologies used to outline static properties like wettability, saturation, porosity, and interfacial tension. Through this exploration, we aim to establish a solid foundation for understanding the reservoir properties and behaviors, laying the groundwork for subsequent discussions.

I-1 Porous Medium

A porous medium is defined as a solid body containing void spaces, termed pores. These pores form a complex network of irregularly-shaped void spaces distributed throughout the material. The porous medium may consist of interconnected or non-interconnected pores.

The distribution and dimensions of pores within the porous medium are irregular, contributing to the variable and complex nature of fluid flow within these materials (Figure I.1). [7].

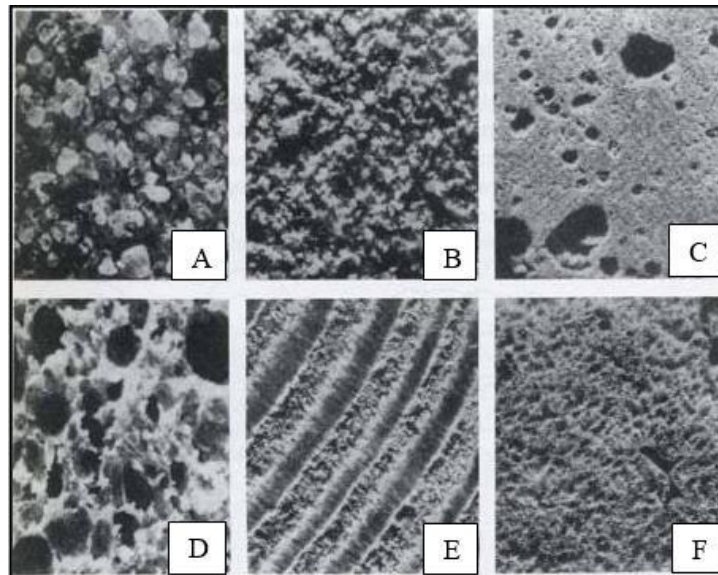


Figure I.1: Examples of porous media ($10 \times$ magnified): (A) beach sand, (B) sandstone; (C) limestone; Dry (D) rye bread; (E) wood; (F) human lung [8].

Key characteristics of a porous medium include the relatively high specific surface area of the solid matrix, which influences fluid behavior, and relatively narrow openings comprising the void space. Interconnected pore spaces facilitate fluid flow, while

unconnected pores may be considered part of the solid matrix. However, certain portions of interconnected pore space may be ineffective for flow, such as dead-end pores with limited connections to the main pore network [7].

I-2 Porous Medium types

I-2-1 Unconsolidated porous media

Characterized by a solid phase composed of grains or fibers that lack cohesion and are not welded together. These grains or fibers, such as gravel, sand, or silt, exist in a loose arrangement within the medium [9].

I-2-2 Consolidated porous media

Refers to a porous medium where the solid matrix is densely packed and composed of cemented grains, such as limestone or sandstone. The individual particles within the matrix are bound together by a cementing material. A distinctive characteristic of consolidated media is their capacity to maintain sample shape under pressure or manipulation [9].

I-2-3 Homogeneous porous media

Characterized by uniformity in flow resistance at any given point relative to a specified direction [9].

I-2-4 Isotropic and anisotropic media

A medium is said to be isotropic when its resistance to flow, or any other property, remains consistent in all directions, irrespective of the direction considered. Conversely, if the medium exhibits variation in properties depending on the direction, it is classified as anisotropic. [9]

Rocks and soils represent the most commonly exploited porous media, with clay layers often forming impermeable walls in natural water or hydrocarbon reservoirs. An aquifer, for instance, serves as a reservoir capable of containing water and facilitating flow, either naturally by gravity or through artificial pumping mechanisms [10].

I-3 Porous medium study scales

For a comprehensive analysis of fluid flow in porous media, it is essential to define the scale of observation precisely; several scales can be distinguished, including:

I-3-1 Molecule Scale

This is obviously the smallest possible element. This scale concerns molecular interactions at particle and pore surfaces. These interactions can influence wetting properties, capillarity, and other aspects of fluid behavior at the microscopic scale.

I-3-2 Particle Scale

Refers to a continuous geometric medium made up of several molecules, but always considerably smaller than a pore in the medium. This scale this refers to the size of the particles making up the reservoir rock. These particles can be grains of sand, clay, etc. Understanding the distribution, shape, and size of these particles is crucial to assessing the rock's permeability and porosity, as well as its potential as an oil or gas reservoir.

I-3-3 Subsystem Scale

Represents a portion of soil (fluid and solid) large enough to present significant average characteristics yet small enough to allow differentiation operations in space. This allows the study of phenomena on an intermediate scale between micro and macro [11],[12].

According to Franck Laurel Nono Nguendjio [13], the global study of a flow is carried out on four scales represented in table (I.1):

Table I.1: Different porous medium scales [13].

Porous medium scale	Scale range
The surface scale	Chemical interactions
The pore scale	In the micron range
The Darcy scale or local scale	In the mm to cm range
The macroscopic scale	In the decimeter to meter range

The pore scale and Darcy scale are the most widely applied for determining the various parameters of porous media: grain size distribution, grain arrangement, and pore size, (Figure I.2)

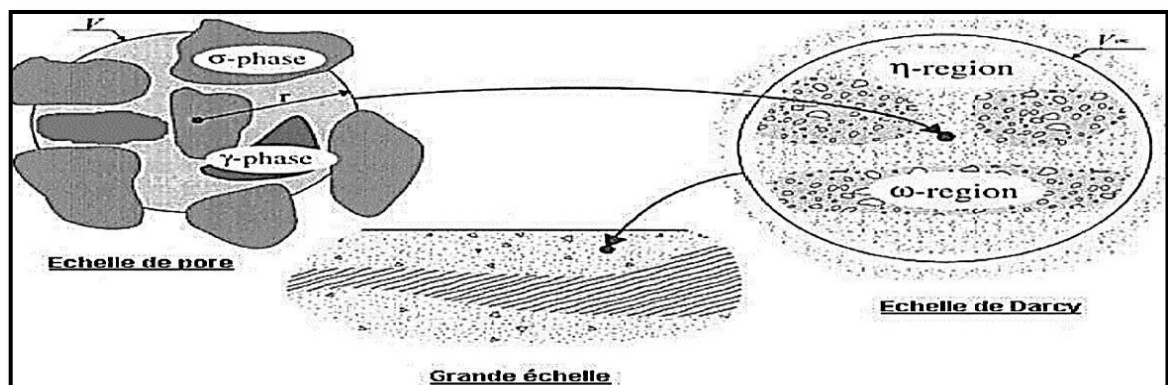


Figure I.2: Different porous medium scales [14].

Instead, at the local scale, relying on Darcy's flow models for single-phase flows and

generalized Darcy's law for polyphasic flows, we will use physical characteristics at the local scale such as porosity, permeability, and saturation [15].

The transition from the pore scale to the Darcy scale involves determining that the Representative Elemental Volume REV that is a volume large enough to estimate the parameters associated with the pore space and small enough to be negligible when describing the macroscopic scale [16].

I-4 Multiphase flow in porous media

The simultaneous path of multiple fluid phases through a permeable material or porous medium is known as multiphase flow. This occurs regularly in many businesses, including gas and oil production, where gas, water and oil flow together. Suspended particles interact with the continuous fluid phase. Like sediment transport in rivers, multiphase flow can also occur. Different chemical components, such as water and water vapor or oil and water, may form the flow. These phases may be discrete (solid, liquid or gaseous) or continuous (gaseous or liquid) [17],[18].

I-4-1 Types of multiphase flow

I-4-1-a Stratified flow

- **Stratified smooth flow**

It is a type of multiphase flow where two or more immiscible fluids occupy different layers within a porous medium or channel. This type of flow is characterized by a smooth interface between the layers, with no significant mixing or turbulence between them. The interface is usually stable and does not exhibit significant vibrations or waves [20].

- **Stratified wavy flow**

A type of multiphase flow characterized by the presence of waves at the interface between two immiscible fluids in a channel or porous medium. These waves create turbulence at the interface, resulting in an undulating pattern that distinguishes it from smooth laminar flow. The behavior of undulating laminar flow is influenced by factors such as interfacial tension, gravity and the relative velocities of the two fluids [21].

I-4-1-b Intermittent Flow

- **Elongated bubble flow**

It is a type of multiphase flow characterized by the presence of elongated gas bubbles within the liquid phase. These elongated bubbles can exhibit a variety of shapes and sizes, affecting the overall flow behavior and transport phenomena in the system [22].

- **Slug flow**

It is a type of two-phase flow, characterized by the intermittent passage of liquid slugs followed by extended gas bubbles flowing through a pipe. This flow regime is similar to slug flow, but the bubbles are larger and flow more rapidly. The presence of slug flow can lead to pressure oscillations within piping systems, which can cause fluid dynamic forces and induce vibrations that can lead to structural damage [23].

I-4-1-c Annular flow

It is a type of multiphase flow system where the gas phase travels in the centre of the pipe or channel, while the liquid phase forms a thin layer along the walls [22].

I-4-1-d Flow with dispersion of gas bubbles

It is a multiphase flow system in which gas bubbles are dispersed within the liquid phase, affecting transport and fluid dynamics phenomena precisely by decreasing the fluidity of the liquid. This phenomenon is characterized by the interaction between individual gas bubbles and the continuous liquid phase, affecting the distribution and behavior of the dispersed phase within the flow system [22].

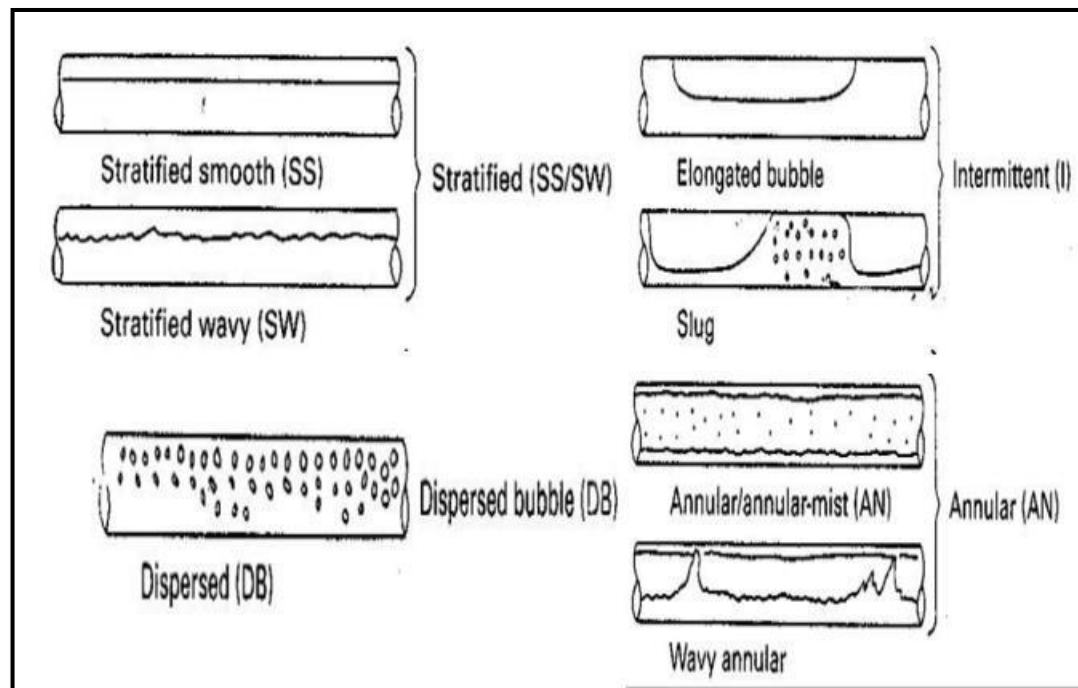


Figure I.3: Multiphase flow types [24].

I-4-2 Multiphase flow in isotropic porous media

Multiphase flow in isotropic porous media exhibits homogeneous flow in all directions. In isotropic porous material, the flow direction is not favored, and the flow routes are consistent throughout. This homogeneity facilitates multiphase flow modeling since the permeability is isotropic, which means it is independent of flow direction. The equations for

multiphase flow in isotropic porous media involve mass conservation for each phase (α) (Equation I-1) and an extension of Darcy's law to explain phase velocities (u_α) (Equation I-2). These equations are fundamental for understanding and simulating fluid behavior in isotropic porous media [25], [26], [27].

$$\frac{\partial(\Phi\rho_\alpha S_\alpha)}{\partial t} + \nabla \cdot (\rho u) = \rho q \quad (\text{I-1})$$

$$u = -\frac{k_{r\alpha} K}{\mu_\alpha} \cdot (\nabla p - \rho g) \quad (\text{I-2})$$

Where:

- Φ is the porosity of the porous medium
- ρ_α is the density of phase α
- S_α is the saturation of phase α
- u_α is the velocity of phase α
- q_α is the source/sink term for phase α
- $k_{r\alpha}$ is the relative permeability of phase α
- μ_α is the dynamic viscosity of phase α
- K is the intrinsic permeability of the porous medium
- p_α is the pressure of phase α
- g is the gravitational acceleration(m/s^2)

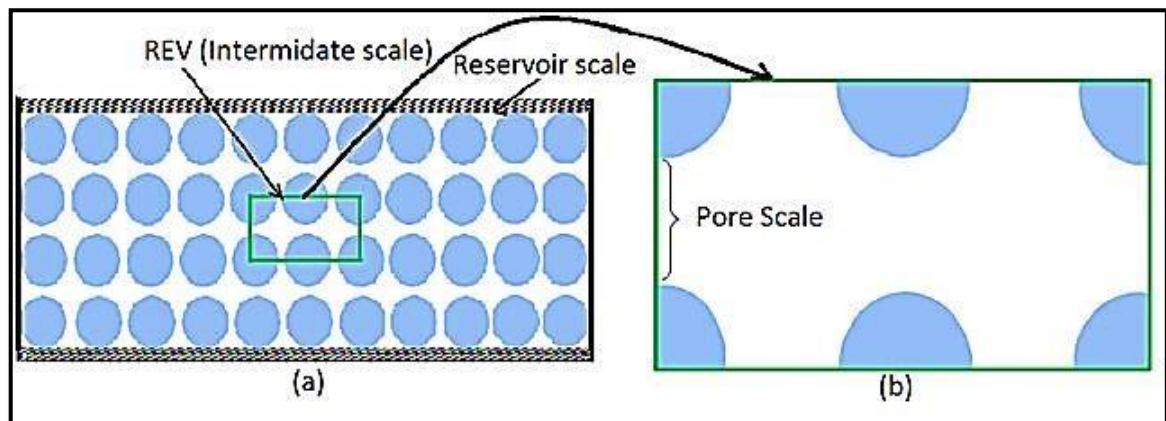


Figure I.4: Schematic diagram of an isotropic porous medium where dark shapes are solids (rocks). (a) An idealized reservoir, and (b) Representative elementary volume [28].

I-4-3 Multiphase flow in anisotropic porous media

Anisotropy occurs when specific characteristics of the porous medium do not have the same value in different directions. The permeability, formation resistivity factor, and

breakthrough capillary pressure in an anisotropic porous material are directionally dependent. In the most common situation, these qualities depend on both placement in the medium and orientation. The probability density function for each attribute can be given with five independent variables: location (x , y , and z) and orientation (θ , ϕ). If the probability density distribution is independent of angular coordinates, the medium is isotropic; otherwise, it is anisotropic. Periodic layering can create anisotropy during reservoir formation (figure I.5). In general, we have distinct characteristics, such as permeability, at the z direction compared to the x and y directions [29].

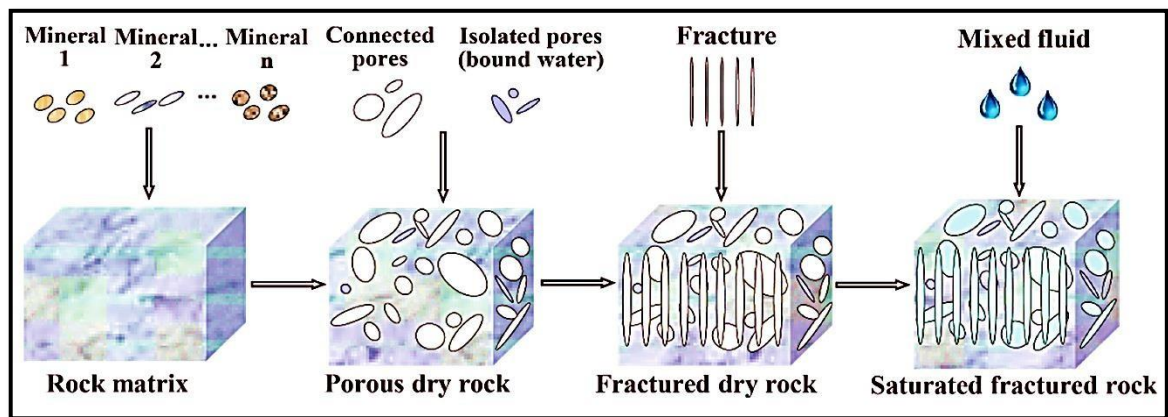


Figure I.5: Anisotropic rock physics modeling flow chart of a fractured tight sandstone reservoir [30].

I-5 Static petrophysical properties

I-5-1 Porosity

Porosity is a small volume or group of pores that fluids can occupy in rocks. The term "pore" in its broadest sense refers to an indiscernible porous space. Cavities are characterized according to their form factor (the ratio of smallest to biggest dimension). In some circumstances, we talk about pores and fissures. In the strictest sense, stomata are convex cavities, whereas fissures are cavities with a very low aspect ratio and insignificant thickness [31], [32]. Bernabé's method, as detailed by Fredrich et al. (1993), characterizes Fontainebleau sandstone, a clay-free granular rock, as having three types of pores in a three-dimensional network. The primary pores, located at grain intersections, form the majority of the pore volume but do not allow fluid flow. Fluid movement occurs when these primary pores are linked by elongated cylindrical voids, termed "tubes" or "fissures," situated between two or three grains. (Figure I.6 and Figure I.7) [33], [34].

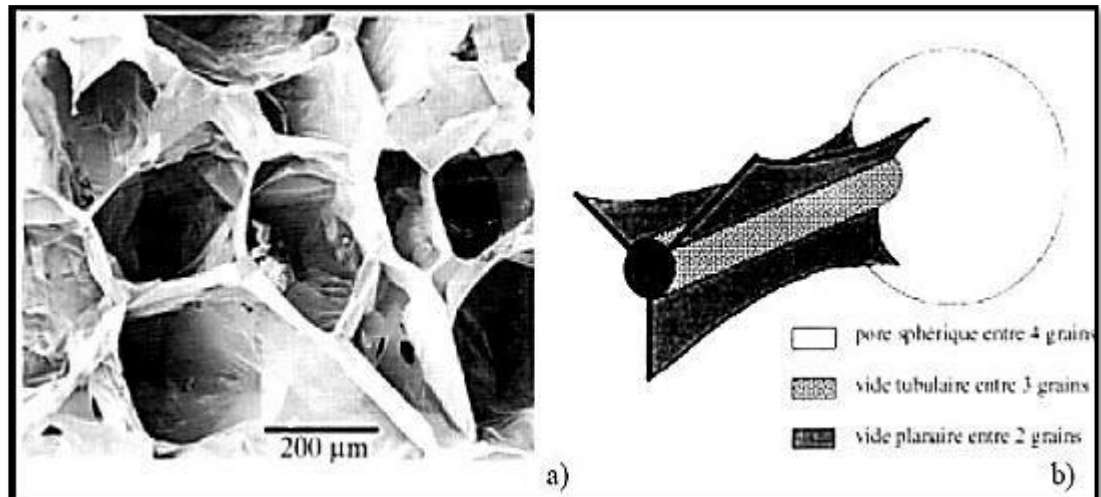


Figure I.6: Porosity in sandstones, a) ME image of the resin-filled pore network of a Fontainebleau sandstone with 4% porosity after acid dissolution of the grains [35], b) Porosity model in sandstone from Bernabé (1991) [33].

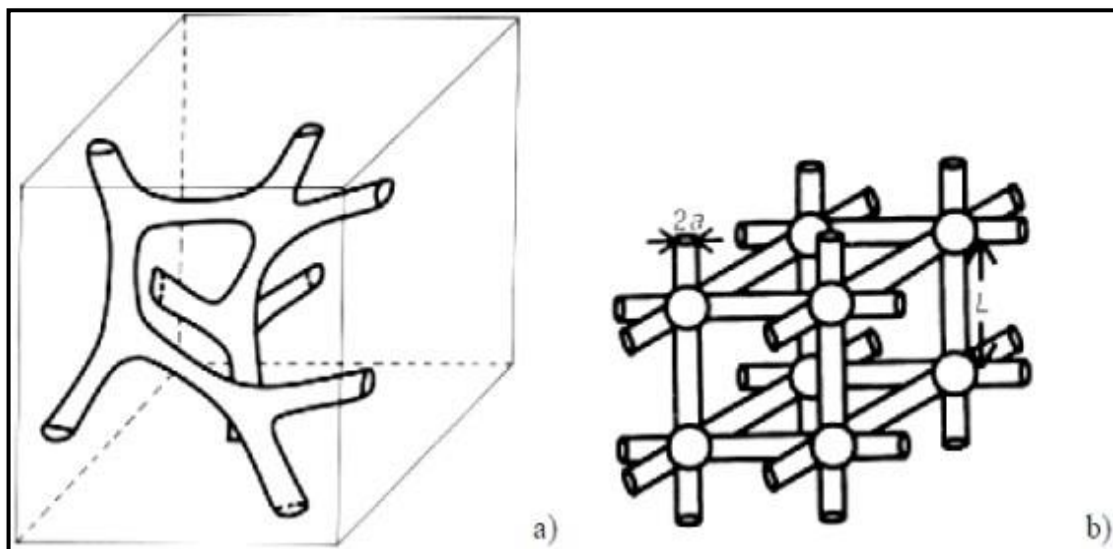


Figure I.7: a) porosity diagram in sandstone [36], b) porous network model (tubes and nodal pores) [37].

I-5-1-a Measure of porosity after crushing and saturation

Crushing a rock yield only the solid matrix and voids between grains. Determine the volume of the solid (V_s) and calculate the using the total volume of rock V (solids + voids). Equation (I-3) gives this result.

$$\Phi = 1 - \frac{V_s}{V} \quad (\text{I-3})$$

When the test sample achieves maximum saturation, the effective porosity or associated porosity can be calculated. To accomplish this, samples are weighed before and

after saturation. Assuming the wetting liquid penetrates the full linked pore space, the mass difference observed is the mass of the liquid, i.e. its density (ρ) multiplied by the pore volume (V_p). If the sample's volume V is known [38], the porosity is given by equation (I-4) below:

$$\Phi = \frac{V_p}{V} \quad (\text{I-4})$$

I-5-1-b Connectivity

A porous medium can have two forms of porosity: total porosity (ϕ_T) and effective porosity. Both are dimensionless and given as percentages. The former is the ratio of void volume to total medium volume, but knowing this does not tell you anything about the voids' dimensions, distribution, or connectedness. The effective porosity (ϕ_E) refers to the porous network through which fluids can flow. Low aspect ratio pores (cracks, grain boundaries, channels) have intrinsic control over fluid flow across the porous network. High aspect ratios and holes at the path's end help to retain fluids effectively (Figure I.8) [39], [40].

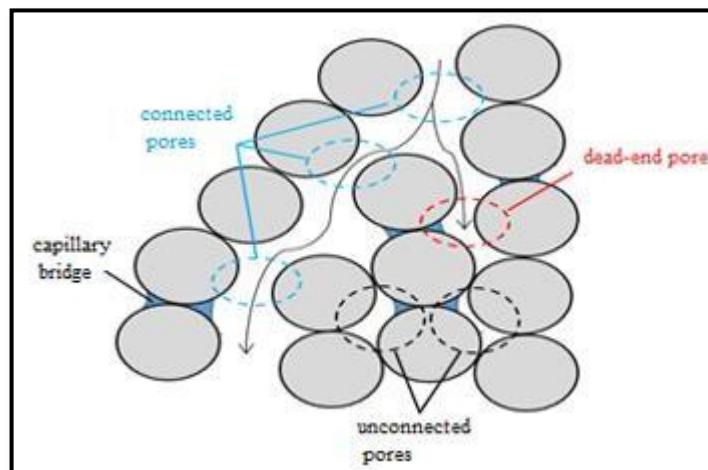


Figure I.8: Different types of pores [40].

I-5-1-c Pore Size Distribution

Pore size distribution in porous media is an important component in determining the pore space within a soil or determination substance. Pores vary in size, ranging from tight constrictions known as pore throats to wider regions known as pore bodies. Pore size distribution is analyzed using a variety of techniques, including mercury intrusion porosimeter and adsorption isotherms. The idea of pore size distribution attempts to reflect the complex geometry of flow channels in porous media, recognizing that pores are interconnected and cannot be easily characterized as separate entities. There is no single definition of "pore diameter" or "pore size," but each method determines a pore size using the pore model that is most suited to the quantity observed in the specific experiment. Pore

spaces are often limited to the pore space confined between solids [29], [41].

I-5-1-d Pore shape

Pore shape assumptions are frequently made, with ellipsoidal or thin spherical pores being the most common. With pore openings serving as pathways for fluid flow inside the porous matrix. The intricacy of pore structures, such as micro nanoscale radii and connectivity, influences hydraulic conductivity and retention capacity in porous media. Understanding pore form is critical for investigating fluid flow, permeability, and other transport phenomena in porous materials (Figure I.9) [42], [43].

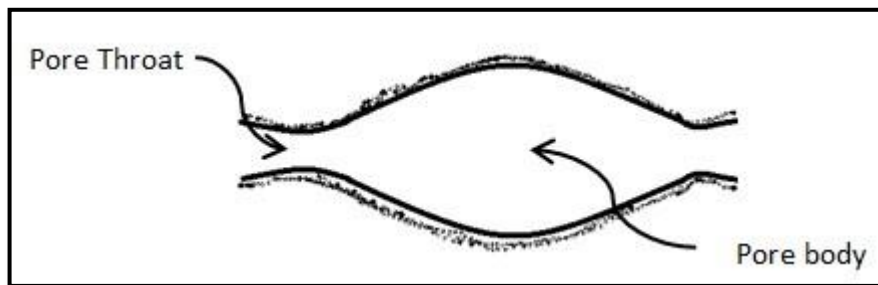


Figure I.9: Schematic representation of pore body and pore throat [41].

I-5-2 Tortuosity

In order to account for the relationship between pores and the complexity of the continuous fluid path through the pores, which affects the medium's transport qualities, we define the tortuosity T . The term "tortuosity" refers to the interconnectivity and sinuosity of the pore space and how it influences the transport processes that occur via porous media [44].

The tortuosity T is a dimensionless number defined as the ratio between the length L' of a current line separating two points and the distance L between these two points (Figure I.10), the tortuosity is mathematically expressed by equation (I-5) as follows:

$$T = \frac{L'}{L} \quad (\text{I-5})$$

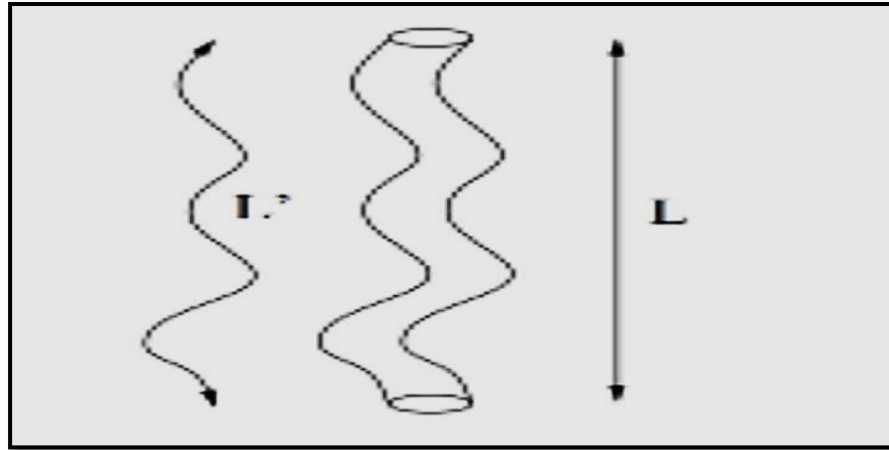


Figure I.10: Diagram of tortuosity [40].

T can also be expressed as a function of the porosity Φ and the formation factor F:

$$T = F\Phi \quad (\text{I-6})$$

Kozeny and Carman related tortuosity to grain size D and permeability K [40], as shown in the formula (I-7):

$$T = AC^2 \frac{D^2}{K} \quad (\text{I-7})$$

Where:

- T represents the tortuosity.
- A is a constant.
- C is the Kozeny-Carman constant.
- D stands for the grain size.
- K represents the permeability.

I-5-3 Saturation

Saturation is defined as the ratio of the volume of a particular fluid to the pore space volume within a rock, Equation (I-8) Usually this is fresh or salt water, but sometimes liquid or gaseous hydrocarbons or other gases (CO_2 , H_2S , etc.) will partially fill these pores.

Porosity, which denotes the capacity of rock to hold fluids, is directly linked to saturation. It represents the total pore space available, while saturation indicates the fraction of this space occupied by a specific fluid. For instance, a water saturation of 10% implies that one-tenth of the pore space is filled with water, while the rest may contain oil, gas, or other substances.

Saturation data is commonly expressed as a percentage and is crucial for estimating the total hydrocarbon volume in place. The thickness of the reservoir rock, along with its

porosity and saturation, influences the overall hydrocarbon reserves. Moreover, knowledge of saturation is essential for determining factors such as recovery potential and production rates, which directly impact the economic viability of a reservoir [45].

$$V_p = V_o + V_w + V_g \quad (\text{I-8})$$

Where:

V_p : pore space volume

V_o : volume of oil

V_w : volume of water

V_g : volume of gas

Therefore:

Water (S_w), oil (S_o) and gas (S_g) saturations are given by equations (I- 9), (I-10), (I-11) respectively:

$$S_w = \frac{V_w}{V_p} \quad (\text{I- 9})$$

$$S_o = \frac{V_o}{V_p} \quad (\text{I-10})$$

$$S_g = \frac{V_g}{V_p} \quad (\text{I-11})$$

The total saturation of the reservoir is constrained by the relationship equation (I- 12):

$$S_w + S_o + S_g = \frac{V_w + V_o + V_g}{V_p} = 1 \quad (\text{I- 12})$$

Furthermore, the concept of hydrocarbon saturation (S_{hc}) is significant, particularly in assessing the presence of oil and gas within a reservoir.

Hydrocarbon saturation is given by formula (I-13).

$$S_{hc} = 1 - S_w \quad (\text{I-13})$$

Where S_{hc} is the hydrocarbon saturation in (%). When the hydrocarbons were introduced into the trap, they displaced a large part of the original water, leaving only a non-displaceable volume of water in the hydrocarbon zone known as irreducible water (S_{wi}) [46],[47].

I-5-3-a Irreducible water saturation

The irreducible saturation (S_{wir}) of a fluid is the minimum saturation of that fluid attainable when that fluid is displaced from a porous medium by another immiscible fluid. Water is typically the wetting fluid in oil or gas reservoirs, so a layer of adsorbed water coats pores surface. Formations at irreducible water saturation cannot produce water until

water invade into the reservoir after some oil or gas has been withdrawn. The surface area-to-volume ratio of pores influences S_{wir} , with smaller pores exhibiting higher irreducible water saturation due to their larger relative surface area. Consequently, in formations with small pores, S_{wir} may reach 1.0, leaving no space for oil or gas accumulation [48].

I-5-3-b Critical oil saturation

For the oil phase to flow, the oil saturation must exceed a certain value, known as critical oil saturation (COS). At this particular saturation, the oil remains in the pores and, for all practical purposes, will not flow. After this saturation, oil will flow [49].

I-5-3-c Residual oil saturation

Oil remaining in the reservoir rock following the flushing or invasion process, or at the end of a specific recovery process (displacing crude oil in the porous medium by injecting or impinging water or gas), is quantitatively characterized by a saturation value exceeding the critical oil saturation. This saturation value is called residual hydrocarbon saturation (S_{or}). The term residual saturation generally pertains to the non-wetting phase when it is displaced by a wetting phase [50].

I-5-4 Interfacial tension

Interfacial tension in porous media has an impact on the liquid pressure required to flow through holes as well as the capillary pressure between immiscible phases (Figure I.11). Interfacial tension is caused by cohesive forces between liquid molecules at the interface. The creation of the contact area ($A_{\alpha\beta}$) between the two phases (α and β) results in a change in the Gibbs free energy (ΔG), as described in equation (I-14) [51],[52],[53].

$$\Sigma\alpha\beta = \left(\frac{\partial G}{\partial A_{\alpha\beta}}\right)_{T, P, n} \quad (\text{I-14})$$

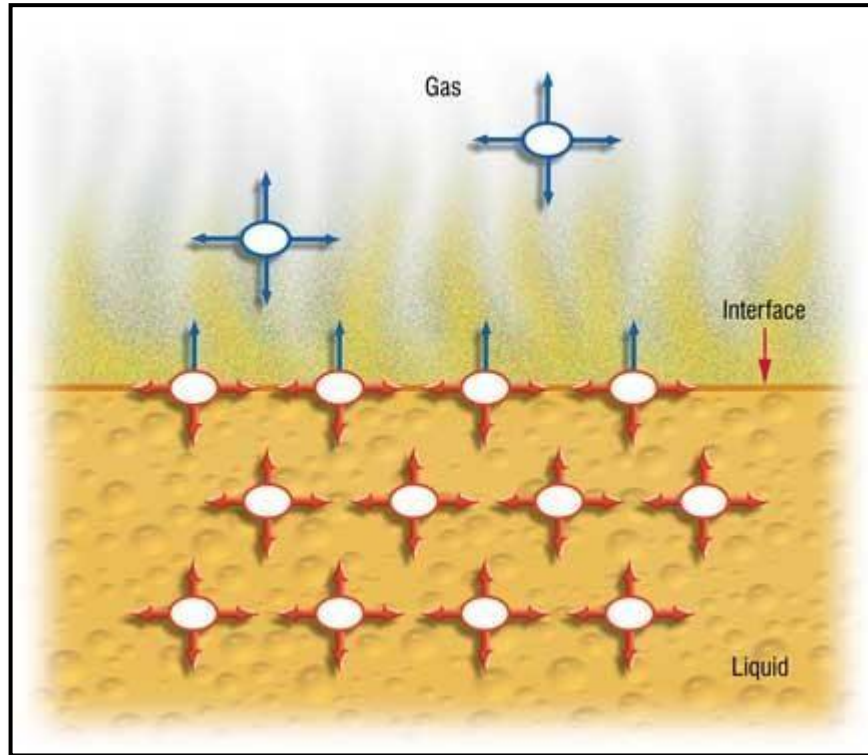


Figure I.11: Intermolecular Forces as They Effect Interfacial Tension [54].

I-5-5 Capillary pressure

Capillary pressure is the difference in pressure between immiscible fluids like oil and water. When a porous medium is saturated with non-wetting Fluid 2 and contacted by wetting Fluid 1, Fluid 1 intrudes, displaces Fluid 2, and achieves equilibrium through imbibitions, where Fluid 1 occupies pore spaces with maximum interfacial curvature (Figure I.12) [55]. The Laplace equation (I-15) can determine the pressure differential known as capillary pressure (P_c).

$$P_c = \sigma_{12} \left(\frac{1}{r_1} + \frac{1}{r_2} \right) = P_{nw} - P_w = P_c = 2\sigma\cos\theta/r \quad (\text{I-15})$$

Where:

- P_c is the capillary pressure,
- σ_{12} is the interfacial tension between the two fluids,
- θ is the contact angle between the fluid-fluid interface and the solid surface (pore wall),
- r is the radius of the pore throat.

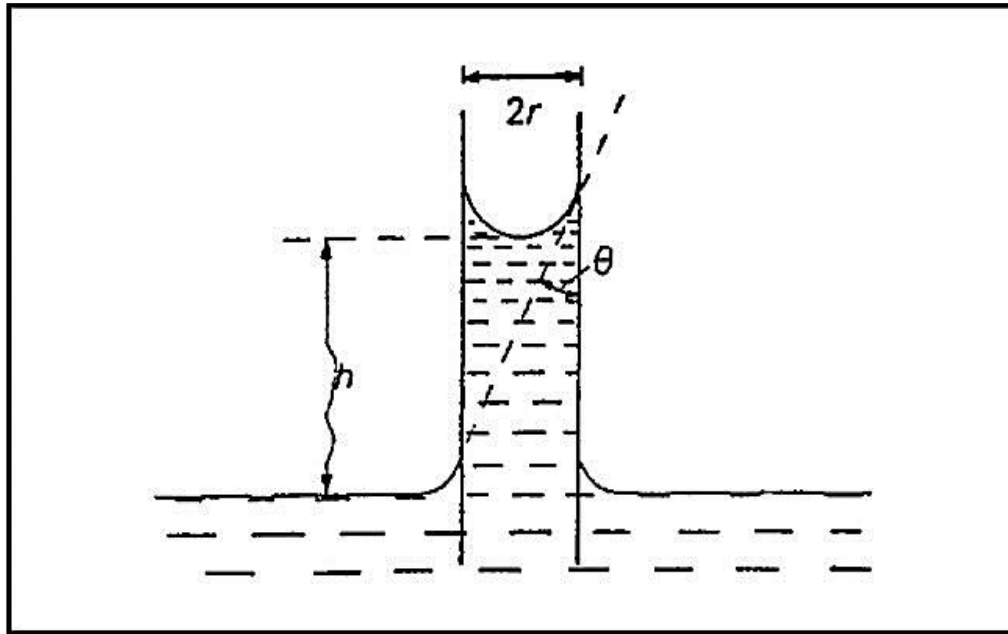


Figure I.12: Rise of liquid in a capillary tube [56].

I-5-6 Wettability

Wettability is the tendency of one fluid to adhere to a solid surface in the presence of another fluid. When two immiscible fluids are in contact with a solid surface, one fluid is usually attracted more strongly than the other fluid. The more strongly attracted phase is called the wetting phase [57]. Wettability results from the interaction of two forces: cohesive forces within the liquid, which work to limit its surface area and keep it in a compact form and adhesive forces between a liquid and a solid, which cause a liquid to spread across the solid surface.

The angle at which the fluid/fluid interface meets the solid surface, is used to quantify wettability. The contact angle for a liquid drop placed on a surface (Figure I.13) [58], follows the Young equation (I-16):

$$\sigma_{ow} \cdot \cos \theta_c = \sigma_{os} - \sigma_{ws} \quad (\text{I-16})$$

With: σ_{ow} , σ_{os} , et σ_{ws} are respectively the interfacial tensions for oil/water, oil/solid and water/solid systems.

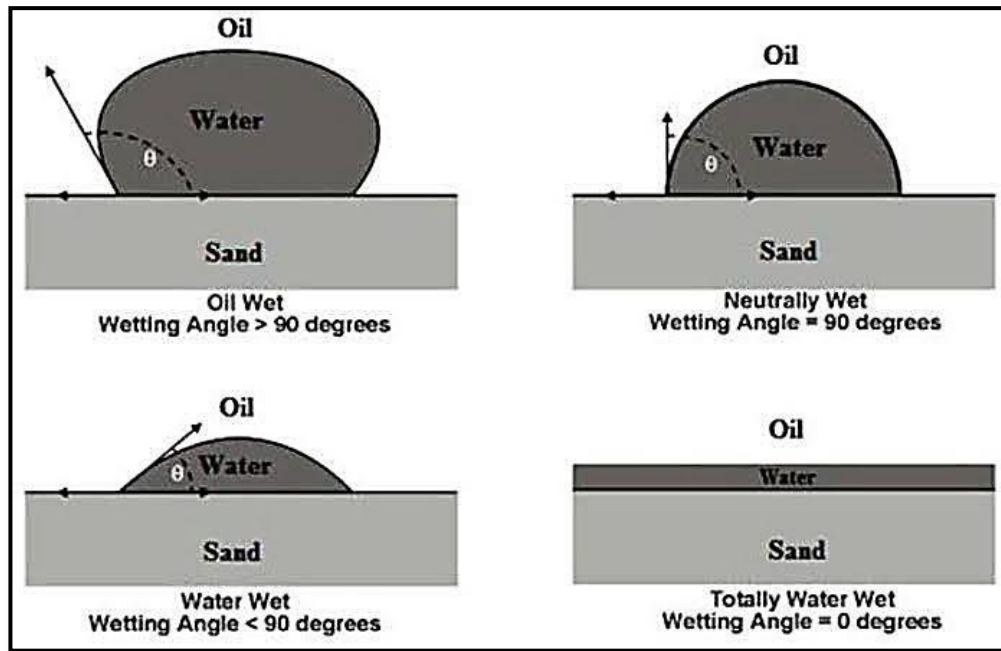


Figure I.13: Wetting Angles for Various Wetting Properties [59].

This describes the other characteristics (interfacial tension and contact angle) and the wetness condition. In the context of multiphase flow at the pore scale, the non-wetting phase is defined as shown in table (I.2) below:

Table I.2: Rock wettability profiles according to the contact angle [60].

Contact angle range	Less than 90°	More than 90°	Nearly 90°
Rock wettability state	Water-wet	Neutral (intermediate) wettability	Oil-wet

I-5-6-a Wettability Classification

➤ Single-phase wettability

Reservoir rocks are generally considered to be water-wettable before the displacement of hydrocarbons by density differences. Water will cover the pore surface and saturate the smaller holes if the medium has a strong affinity for it, whereas droplets of oil will be detected in the middle of the bigger pores. The liquid distribution in a frank oil wettability situation is the reverse of a frank water wettability situation. The oil covers the surface of the large pores and saturates the microscopic pores. The adsorption of some of the molecules that comprise the crude oil on the grain surface causes the state of frank wettability with oil. The various interactions between the rock matrix, the aqueous phase, the oil phase, and its components give rise to different types of wettability.

The wetting state turns neutral if the rock has no affinity for either the water phase or the oil phase [61].

➤ Fractional Wettability

The notion that diverse forms of wettability exist in reservoir rock was inspired by the discovery that adsorbable crude oil components can change the wettability of rock. Brown and Fatt [62] suggested fractional wettability, often known as heterogeneous and spotted wettability. When there is fractional wettability, some parts of the rock are strongly adsorbed with crude oil components, making that piece of the rock strongly oil-wet and the remaining portion strongly water-wet [63].

➤ Mixed wettability

Mixed wettability is a condition where both oil and water can wet the rock surface simultaneously. This can be seen in systems where smaller pores are water-wet and filled with water, while larger pores are oil-wet and filled with oil.

Interest in wettability arises from its significant impact on the distribution of immiscible fluids in porous media and the impact of this distribution on the movement of these fluids [64], (Figure 1.14) shows the different states of wettability in porous media.

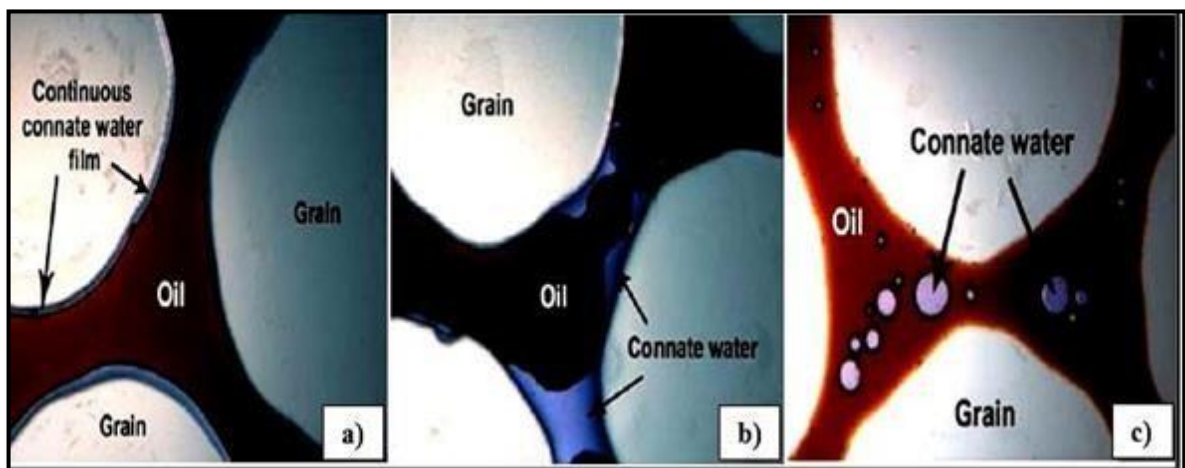


Figure 1.14: Types of wettability in porous media: a) Free water wettability, b) Fractional wettability, c) Free oil wettability [65].

Conclusion

To conclude this chapter in which we provided an overview of porous media and conducted a bibliographic search covering their various classifications, multiphase dynamic flow phenomena, and their basic petrophysical properties. We have studied the critical role of factors such as porosity, permeability, saturation, surface tension, and wettability in controlling the behavior of fluids within porous media.



Chapter II

*Preferential flow pathways and oil
recovery strategies*

Introduction

This chapter delves into the dynamic fluid behavior within porous media, encompassing fundamental concepts such as reservoir relative permeability, its measurement techniques, and advanced oil recovery strategies. Through a comprehensive examination, the aim is to unravel the intricate relationship between pore geometry and oil recovery, investigating the ways in which fluid preference flow paths impact the multiphase flow, recovery and phase trapping in reservoir pores. As well as to clarify the complexities of fluid flow in porous media and provide insight into innovative strategies for optimizing hydrocarbon recovery.

II-1-Permeability

The term "permeability" refers to a rock's capacity and ability to transmit fluids. Which is influenced by the size, shape, distribution, packing, and level of cementation and consolidation of the grain? It controls also the directional movement and flow of the reservoir fluids.

Permeability is also influenced by the kind of cementations material or clay that lies between the grains of sand, especially in areas where freshwater is prevalent. Certain clays, especially smectites and montmorillonites, have a tendency to swell in fresh water, seep partially or entirely into the sand, and subsequently partially or totally clog pores [66].

In 1856, Henry Darcy investigated the flow of water through sand filters for water purification, he observed that the flow rate of water is proportional to the cross-sectional area of the sand pack A , the pressure difference and its length and to convert this proportionality to an equation (Equation II-1), a constant K must be introduced, which was found to be characteristic of the sand pack.

$$Q = K \cdot A \cdot \frac{\Delta P}{L} \quad (\text{II-1})$$

Darcy's investigations were confined to the flow of water through sand packs, which were entirely saturated with water.

Later, investigators found that it could be extended to other fluids as well as water by splitting the constant K into a component k , which is a property of the sand pack (or rock) and the viscosity of the fluid.

At the first World Oil Congress in 1933. The equation (II-2) was named Darcy Law. And the constant k was termed permeability [57]. Hence, the equation becomes:

$$Q = \frac{k}{\mu} \cdot A \cdot \frac{\Delta P}{L} \quad (\text{II-2})$$

Where:

Q: Flow cm^3/s .

k: Permeability of porous rock, Darcy, 1 darcy = 1 (μm^2).

A: Cross-sectional area of rock, cm^2 .

μ : Fluid viscosity, centipoises (cP).

L: Length of rock sample, cm.

ΔP : Deferential pressure (atm).

The unit of permeability is called Darcy (D). For most reservoirs, the permeability is less than 1 Darcy; therefore, it is common to use md [57].

The range of permeability's encountered is very wide, from 0.1 mD to over 10 D, the following table II.1 can be used to specify the permeability values [67]:

Table II.1: Permeability range classification [67].

Permeability values range	Classification terms
< 1 mD	Very low (Tight)
1 to 10 mD	Low
10 to 50 mD	Poor
50 to 200 mD	Average
200 to 500 mD	Good
> 500 mD	Excellent

II-1-1 Absolute permeability

The permeability, k_a in the equation (II-2) is called the “absolute” permeability or specific permeability, is defined when only a single fluid or phase flows through a porous medium, the rock is 100% saturated with it [68].

II-1-2 Effective permeability

In practice, in hydrocarbon deposits, there are always at least two fluids present (water and hydrocarbons). Darcy's law can then be used to define an effective permeability for each fluid. (k_{effo} , k_{effg} , or k_{effw} being oil, gas, or water effective permeability, respectively).

The effective permeability of a rock refers to its ability to allow a specific fluid to flow when other immiscible fluids are present.

Reservoir fluids interface with each other during their movement through the porous

channels of the rock. Consequentially, the sum of the effective permeability's of all the phases will always be less than the absolute permeability [66], [67].

II-1-3 Relative permeability

In the presence of more than one fluid in the rock, the ratio between the effective permeability of any phase and the absolute permeability is called the “relative” permeability (k_r) of that phase [66].

On this basis, relative permeability is given by the following equation (II-3):

$$K_{r_i} = \frac{K_{eff}}{K_a} \quad (II-3)$$

Where:

i : represents the fluid phase oil, water or gas.

K_{eff} : represents the relative permeability

K_a : represents the absolute permeability

II -1-4 Permeability Classification according to the origin and formation process

II-1-4-a Primary permeability

Primary permeability, also referred to as matrix permeability, is the permeability that originates during the deposition and lithification (hardening) processes of sedimentary rocks. This type of permeability is inherent to the rock formation and is established at the time of its formation [66].

II-1-4-b Secondary permeability

Secondary permeability, on the other hand, arises from the subsequent alteration of the rock matrix. This alteration can be caused by various geological processes, such as: Compaction, Cementation, Fracturing and Solution. In some reservoir rocks, particularly low-porosity carbonates, secondary permeability is the main flow path for fluid migration [66].

II -1-5 Factors affecting permeability

➤ **Shape and size of rock grains**

They significantly impact the permeability of a rock. Large, flat grains aligned horizontally (FigureII-1-A) result in high horizontal permeability and medium-to-large vertical permeability. In contrast, large, rounded grains (FigureII-1-B) lead to high permeability in both directions. Small, irregularly shaped grains (FigureII-1-C) typically result in lower permeability, particularly in the vertical direction, which is common in petroleum reservoirs. These reservoirs are classified as anisotropic due to their directional

permeability, which significantly influences fluid flow characteristics. The difference in permeability between parallel and vertical directions to the bedding plane is primarily due to the sediment's origin, where grains settle with their longest and flattest sides in a horizontal position. Subsequent compaction further enhances the ordering of grains, resulting in a general alignment in the same direction [69].

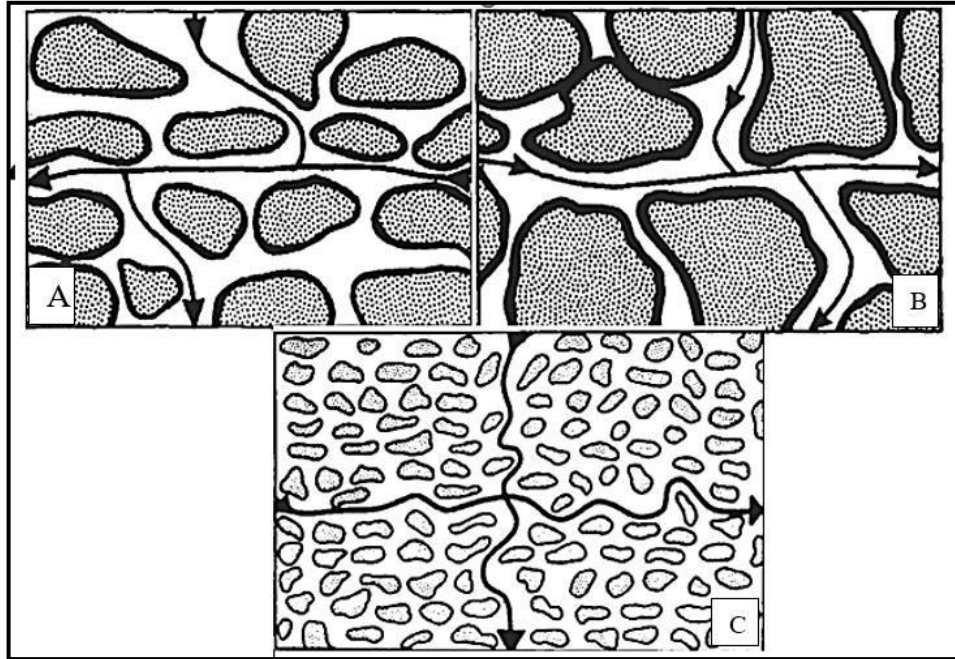


Figure II.1: Effects of grains shape and size on permeability: A. Large, Flat Grains, B. Large, Rounded Grains, and C. Very Small Irregular Grains [69].

➤ **Lamination**

As minerals and shale layers, can impede permeability by obstructing fractures, jointing, and vertical solution channels when filled with clay or other minerals. The significance of clay minerals in regulating permeability is not solely tied to their prevalence but also to their mineralogical characteristics and the composition of pore fluids. If clay minerals covering grain surfaces undergo expansion or detachment due to alterations in pore fluid chemistry or infiltration of mud filtrates, a substantial decrease in permeability is expected [66].

➤ **Cementation**

Figure (II-2) illustrates how the degree of cementation and the placement of the cementing material, in addition to its precipitation inside the pore space, affect the permeability and porosity of sedimentary rocks. Where the grains without clay (a) perform a higher permeability ($K_h = 1000$ mD, $K_v = 600$ mD) than the grains with clay (b) ($K_h = 100$ mD, $K_v = 25$ mD).

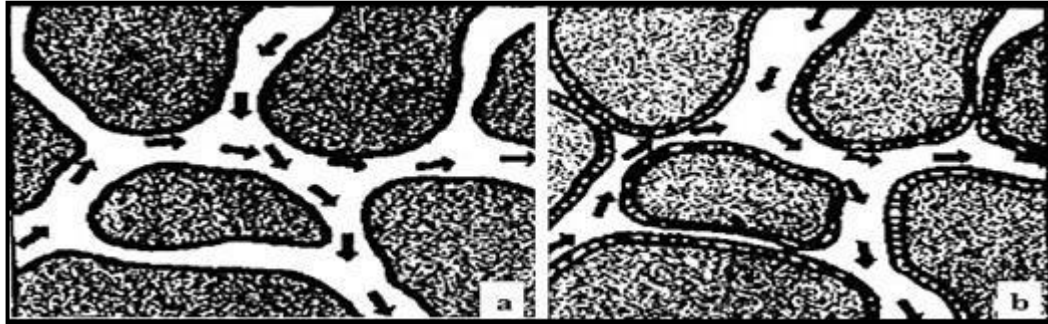


Figure II.2: Effects of clay on permeability: a. Sand grains without clay, b. Sand grains with clay [70].

➤ Solution and fracturing

In sandstone rocks, fracturing is not a significant factor contributing to secondary permeability, with the exception of situations in which sandstones are bound together with dolomites, shale's, and limestone regarding carbonates.

The permeability of the reservoir rock is increased by the dissolution of minerals that are carried by surface and subsurface acidic waters as they move through primary pores, which can enlarge existing pore spaces or create new ones, thereby increasing permeability. The development of cracks and fissures within the rock creates additional pathways for fluid flow [71].

II -1-6 Permeability measurements

There are two methods for determining relative permeability's the unsteady-state method (displacement method) and the steady-state method (Permanent flow method).

Displacement Method

The relative permeability calculation relies on the work of Buckley & Leverett (1942) [72], with additions provided by Welge (1942) [73] to ascertain the average saturation downstream of the displacement front and the saturation value of the displacement front. One liquid is replaced with another to take measurements. Darcy's velocity equation and those found in the literature, including the JBN approach [74], and are used to compute the properties on the flow's outlet side.

Consider a homogeneous medium with the following characteristics: A is the cross-sectional area, L sample length, Φ porosity with irreducible water saturation. The method is based on the displacement of oil by water at a constant flow rate.

Water is injected through the plug. The oil is displaced first, however, just after the water breakthrough; both oil and water are produced at the same time. The method is called unsteady state because the saturations of the two phases change throughout the water

injection. If a constant flow rate is used, the pressure drop across the sample will change as the proportion of flowing brine increases, and if a constant flow pressure is used, both phase saturation and flow rate will increase [75], the process is shown in (figureII.3).

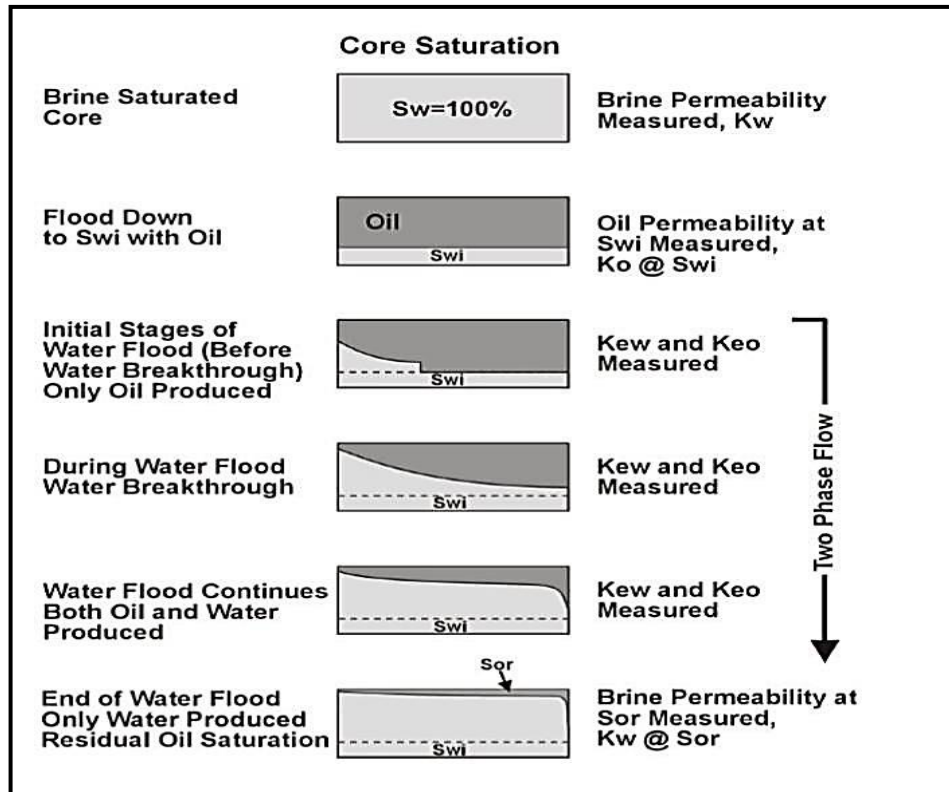


Figure II.3: Schematic illustration of an unsteady state relative permeability determination method [76].

Permanent flow method

The steady-state relative permeability test is a method used to determine the permeability of oil or water in a mixture, schematically illustrated in (figureII.4). It involves determining the porosity of the sample, flushing oil through a saturated core, and calculating the permeability of the core to oil using the Darcy's Law. Oil and water mixtures of varying proportions are then flushed through the core, with the final flush being with brine to obtain the permeability at residual oil saturation. The test continues at a constant flow rate until a constant differential pressure is achieved, typically one to three days. The permeability's of oil or water are calculated using the pressure drop across the core and the flow rate of each phase. Samples are typically enclosed in heat shrink wrap or tubing to limit errors due to fluid evaporation or grain loss. Thorough mixing of the oil/water mixture is provided by mixing heads at each end of the sample. Commercial laboratories usually obtain steady-state data at five saturation points, including residual water and residual oil saturation [75].

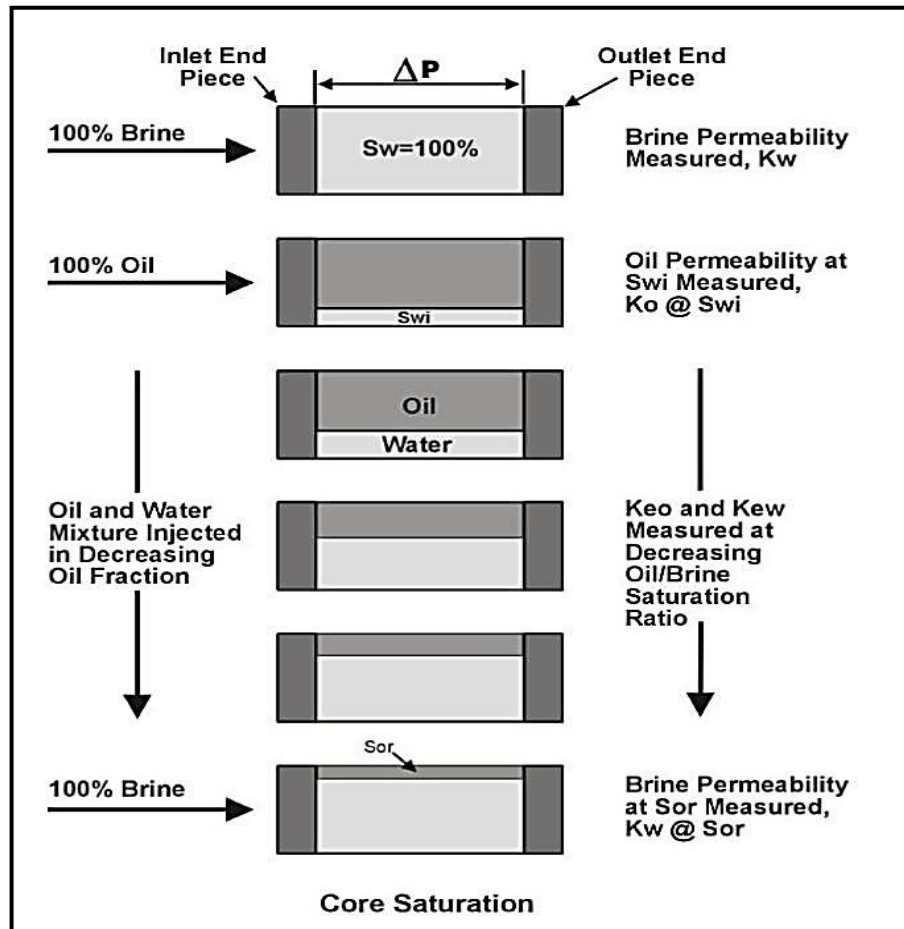


Figure II.4: Schematic illustration of a steady state relative permeability determination method [76].

II-1-7 Effect of wettability on relative permeability

Relative permeability's for water-wet and oil-wet rocks have been extensively studied. (Figure II.5) illustrates two common trends in relative permeability curves, where the performance of relative permeability's is plotted against the water saturation of the system. A quick, qualitative analysis of rock wettability is performed based on the point of intersection between the water and oil relative permeability curves. It had shown that rock is highly wettability to water when the point of intersection between the relative permeability to water and that to oil is above 50% of water saturation. For highly oil-wettable rock, the point of intersection of the two relative permeability curves is less than 50% of water saturation. When the point of intersection of the two relative permeability curves is at 50%, it represents the forehead of displacement [68].

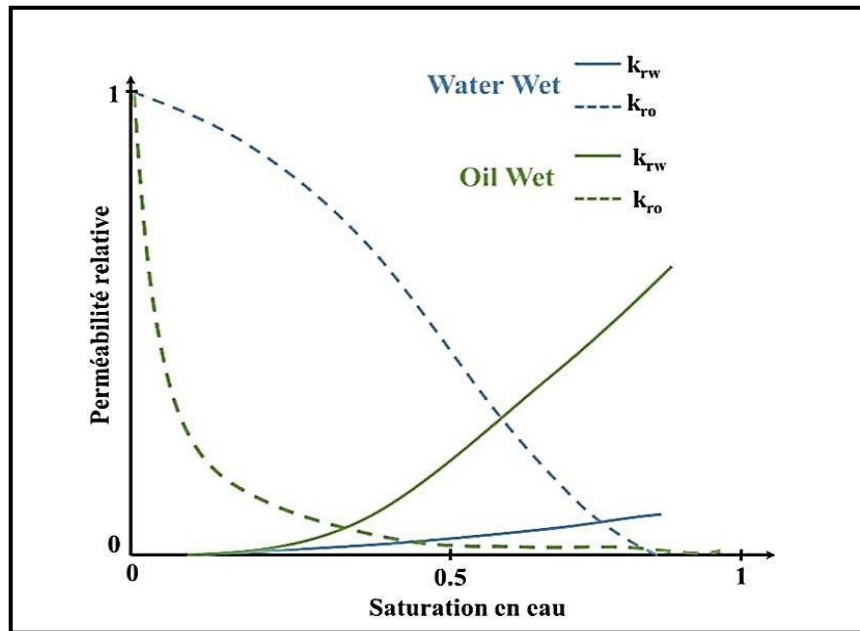


Figure II.5: schematic representation of the relative permeability curve [68].

In oil-wet systems, the relative permeability of oil (k_{ro}) significantly decreases while the curve of relative water permeability (k_{rw}) increases rapidly. This occurs because oil tends to wet the rock surface in larger pores, while water readily displaces the oil present in these areas. In such systems, k_{rw} can reach values greater than 0.5 (Figure II.6) [76].

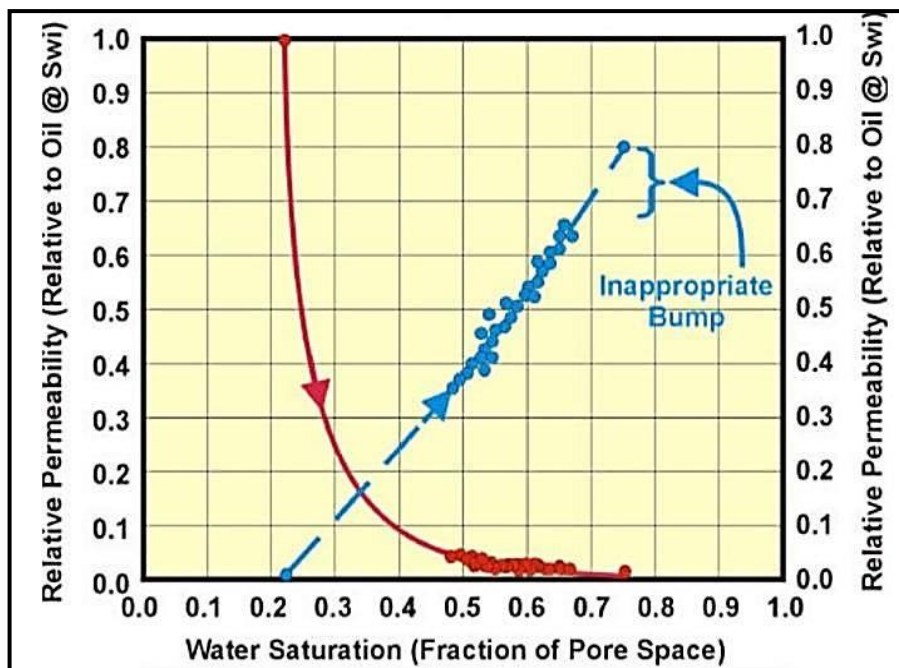


Figure II.6: Typical relative permeability curves of an oil-water pair for an oil-wet system [76].

Conversely, in water-wet systems, water prefers to remain in smaller pores, leading to a tendency for k_{rw} to remain low. Conversely, oil becomes trapped in larger pores, blocking

the main flow channels. Therefore, when water is injected, oil will be continuously produced until water starts to significantly bypass the residual oil, thereby increasing the residual oil saturation. This type of system typically retains between 20 and 50% of the original oil in place. (Figure II.7) [76].

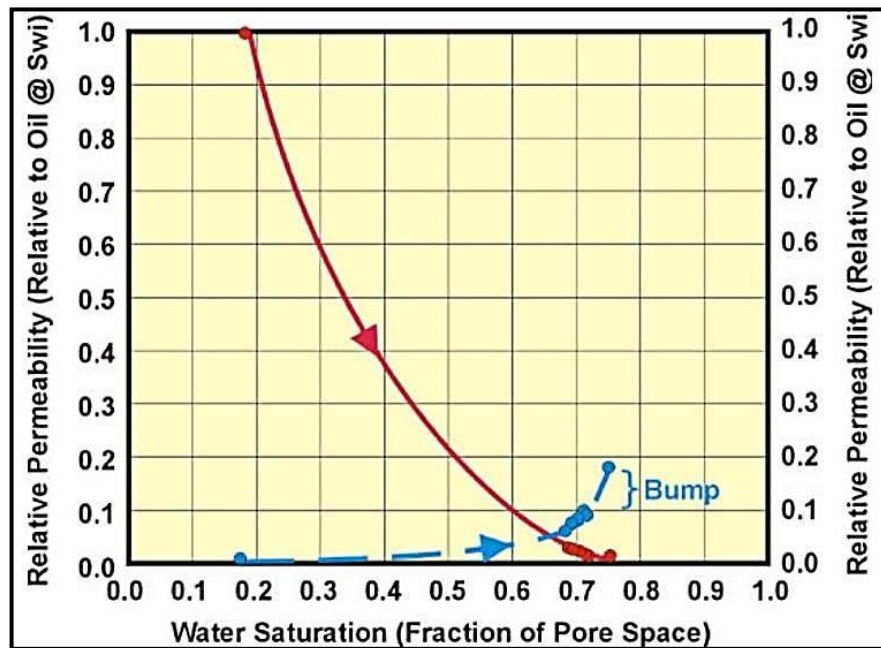


Figure II.7: Typical curves for the relative permeability of an oil-water pair for a water-wettable system [76].

II-1-8 Effect of capillary number on relative permeability

At the pore scale the ratio of viscous forces to capillary forces, or the capillary number Ca , is used to represent the trapping phenomenon. (Equation II- 4):

$$Ca = \frac{\eta v}{\sigma} \quad (\text{II-4})$$

With: η is the viscosity of the displacing fluid, v is the fluid velocity, σ is the interfacial tension between water and oil; this is typically 50mN/m which corresponds to a capillary number of 10⁻⁸. Thus, low capillary number values are the conditions under which the two-phase flow regime (oil/water) occurs within porous media [77].

R.A. Fulcher, Jr. conducted series of relative permeability measurements to determine whether the capillary number causes changes in the two-phase permeability's or whether one of its constituents, such as flow velocity, fluid viscosity, or interfacial tension (IFT), is the controlling variable.

The results of the experiment demonstrated a relationship between the capillary number and the relative permeability of the no wetting phase (oil). The oil permeability

sharply rose when IFT dropped. On the other hand, the oil's flow decreased as the viscosity of the water rose. The opposite capillary number effect was seen for the wetting-phase (water) relative permeability. The water permeability rose for both the tension reduction and the viscosity rise (i.e., an increase in capillary number). On the other hand, the increase in the oil curves with a decrease in IFT was greater than the increase in water. There were no observed velocity effects [78].

II-2 Preferential flow path

Preferential flow paths are channels or pathways inside porous media that fluids prefer to follow for a variety of reasons, including the medium's structure, the fluids' characteristics, and pressure gradients. These channels are critical in oil recovery procedures because they influence fluid movement and distribution within the reservoir, which affects total extraction efficiency characterizing optimal flow routes is critical for optimizing oil recovery techniques because it identifies places where fluids are more likely to flow and where injection strategies can be targeted to maximize oil recovery (Figure II.8).[79].

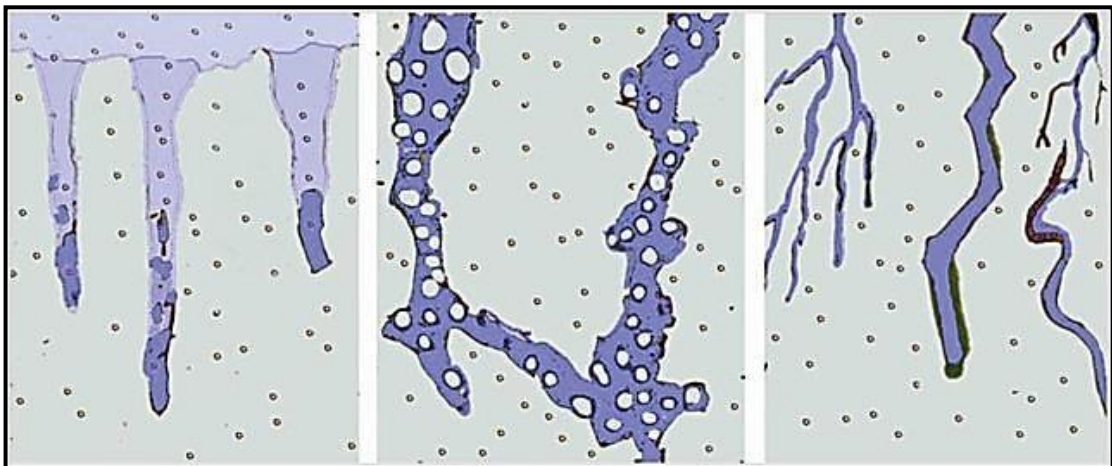


Figure II.8: Conceptual drawing of three types of preferential flow [80].

II-3 Oil recovery

Oil recovery, also known as petroleum recovery or oil production, is the extraction of crude oil from subsurface reservoirs for a variety of industrial and commercial applications. It entails a variety of strategies targeted at increasing the amount of oil that can be retrieved from a reservoir.

II-3-1-Primary recovery

Primary recovery is the first stage of oil extraction such as gas drive, water drive or gravity drainage that uses natural reservoir pressure to force oil to the surface without external assistance (figure II.9). It normally recovers approximately 10% of the oil in a well.

Primary recovery is limited when reservoir pressure falls to an economically viable level or when the production stream contains a substantial proportion of gas or water. The primary recovery is expressed mathematically by Darcy's law [81], [82], [83].

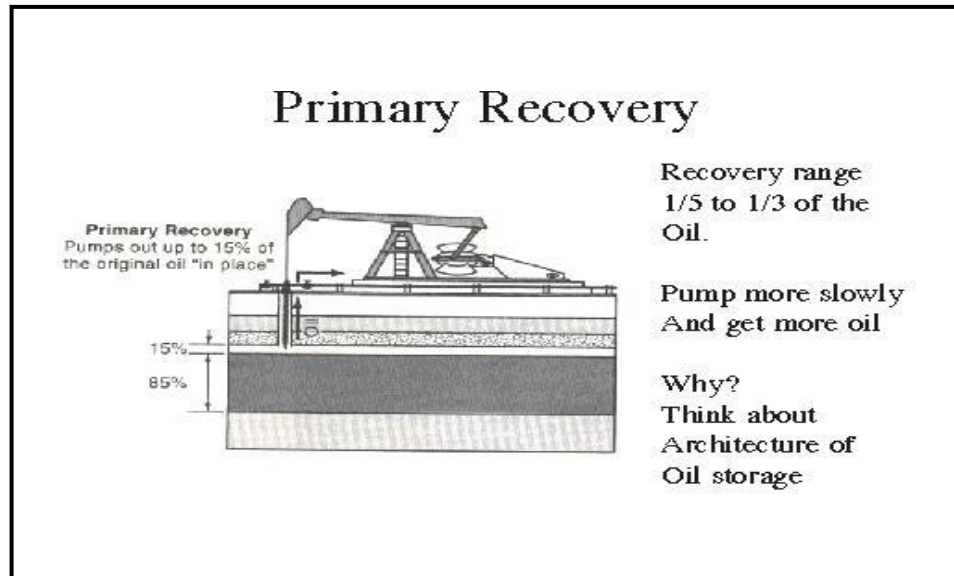


Figure II.9: Primary recovery [84].

II-3-2-Secondary recovery

Secondary recovery in reservoir engineering refers to approaches for increasing hydrocarbon recovery after first recovery. These procedures aim to maintain reservoir pressure while displacing hydrocarbons towards the wellbore. Water flooding and gas flooding are two common procedures for secondary recovery. Water flooding is an immiscible displacement procedure where water is pumped into the reservoir to transport oil to producing wells. Gas flooding can be immiscible or miscible, depending on the procedure (Figure II-10). Secondary recovery can produce 15% to 40% of the original oil in place. Fluid injection techniques, including water flooding, liquid hydrocarbon injection, and in-situ combustion, are used to increase recovery rates. The choice of procedure depends on characteristics such as oil viscosity, rock porosity, and reservoir depth [85], [86], [87]. In its simplest form, the material balance (equation II-5) can be expressed as:

$$N_p = \frac{OOIP - R_{fw}}{RF} \quad (\text{II-5})$$

N_p : is the cumulative oil production.

OOIP: is the original oil in place.

R_{fw} : is the formation water produced.

RF: is the recovery factor.

II-3-2-a Water flooding

Water flooding involves injecting water into reservoirs to displace hydrocarbons and push them towards production wells. The injected water, acting as a driving force, helps push oil towards the production wells, increasing hydrocarbon recovery rates. This method maintains reservoir pressure, maximizes oil displacement and improves production efficiency. Petroleum engineers meticulously design water flooding operations to ensure effective reservoir sweep, minimize steering and maximize ultimate oil recovery [85], [87].

II-3-2-b Gas Flooding

Gas flooding involves injecting gas, often carbon dioxide (CO₂) or natural gas, into reservoirs to support hydrocarbon recovery. By displacing oil and mobilizing it towards production wells, the injected gas acts as a driving force to improve extraction efficiency. Gas flooding operations aim to maintain reservoir pressure, reduce fluid viscosity and improve oil displacement. Consideration of reservoir parameters, gas injection rates, fluid properties and geological heterogeneity is essential to the effective design and execution of gas flooding projects, helping to ensure maximum hydrocarbon recovery while minimizing operational risks and environmental impacts [86], [87].

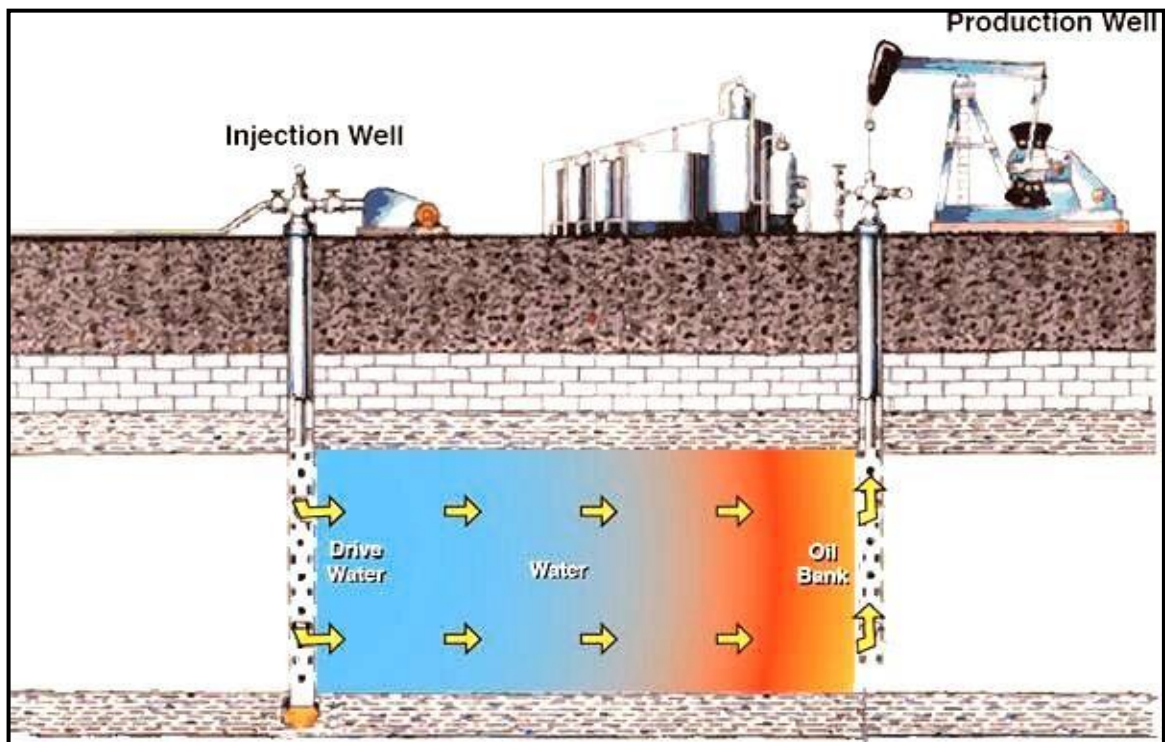


Figure II.10: Illustrating water flooding technique of secondary recovery [88].

II-3-3-Tertiary Recovery

Tertiary recovery, also known as Enhanced Oil Recovery (EOR), is used in formations

with low recovery factors and producing wells that have lost efficiency due to aging. Tertiary recovery entails altering the physical and chemical properties of rocks and formation fluids in order to recover the remaining crude oil underground. Tertiary recovery uses advanced techniques including thermal recovery, gas injection, chemical flooding to increase oil recovery rates, and steam-assisted gravity drainage as shown in Figure II.11. Tertiary recovery aims to maximize the amount of crude oil recovered from reservoirs; especially as standard recovery techniques reach their limits. Tertiary or EOR methods, such as chemical injection, thermal extraction and gas injection, can recover an additional 5% to 20% of the crude oil recovered from the reservoir [89], [90], [91], [92]. (The equation II-6) for tertiary recovery vary on the specific EOR approach being used.

$$EOR = (RF_{EOR} - RF_{secondary}) \times OOIP \quad (II-6)$$

EOR: is the additional oil recovered through EOR methods.

RF_{EOR} : is the recovery factor achieved with EOR.

$RF_{secondary}$: is the recovery factor achieved with secondary recovery methods.

II-3-3-a Thermal enhanced oil recovery

Thermal enhanced oil recovery (EOR) strategies rely on the use of heat to enhance the extraction of heavy and viscous crude oil from reservoirs, especially those with challenging characteristics such as high oil viscosity and low permeability. One widely used approach involves steam injection, where steam is introduced into the reservoir to heat the oil, reducing its viscosity and improving its mobility for extraction through production wells. In-situ combustion is another method that utilizes the injection of air or oxygen to ignite the oil, generating heat and creating a combustion front to push the oil towards production wells. Thermal EOR techniques also increase reservoir expansion, which helps displace oil. However, successful implementation requires careful reservoir analysis, temperature monitoring and operational management to mitigate potential risks such as steam penetration and damage to petroleum reservoirs [89],[90].

II-3-3-1-a Steam injection method

Steam injection is an advanced thermal Enhanced Oil Recovery (EOR) technique that injects steam into oil reservoirs to lower viscosity and improve mobility. It is especially useful for heavy or ultra-heavy oil. It can obtain a recovery factor of 50-60% OOIP, which is much greater than hot water injection. Technological advancements such as nitrogen thermal foam flooding and the use of nanoparticles and biopolymers can help to increase efficiency even further. Key issues include regulating steam override, reducing thermal

energy losses, and maintaining efficient steam generators, therefore operational and economic considerations are crucial for effective adoption [93].

The thermal energy Q needed to be transferred to heat a reservoir during steam injection is determined by the equation (II-7) the oil production rate q_o during a steam drive process can also be calculated by equation (II-8):

$$Q = V_b M_R \Delta T \quad (\text{II-7})$$

$$q_o = \phi \cdot \frac{dV_s}{dt} \left(\frac{S_{oi}}{B_{oi}} - \frac{S_{ors}}{B_{os}} \right) \quad (\text{II-8})$$

Where:

- Q : Heat energy transferred (Joules, J).
- V_b : Bulk volume of the reservoir (cubic meters, m³).
- M_R : Volumetric heat capacity of the reservoir (J/m³·°C).
- ΔT : Temperature difference between the injected steam and the reservoir (°C).
- q_o : Oil production rate (m³/s).
- ϕ : Porosity of the reservoir (%).
- dV_s : Rate of change of the steam swept volume (m³/s).
- S_{oi} : Initial oil saturation (%).
- B_{oi} : Initial oil formation volume factor.
- S_{ors} : Residual oil saturation after steam drive (%).
- B_{os} : Oil formation volume factor after steam drive.

Challenges in steam flooding incorporate steam abrogate and extreme nuclear power misfortunes, which can happen because of misfortunes in surface lines, steam section into wells, and inside the supply. Optimal steam flooding necessitates certain criteria as follows [93]:

High viscosity oil: Steam flooding is very successful in reservoirs with heavy or ultra-heavy oil because the thermal energy from the steam significantly reduces oil viscosity, enhancing flow.

Steam quality: The steam quality, or the ratio of steam to water, is crucial. High-quality steam (with a higher steam concentration) is preferred to maximize thermal efficiency while reducing the amount of water produced alongside the oil.

Heat management: Proper heat management is critical. This includes reducing heat losses in surface lines, maintaining proper steam injection temperatures, and managing heat distribution inside the reservoir to avoid steam override and channeling problems.

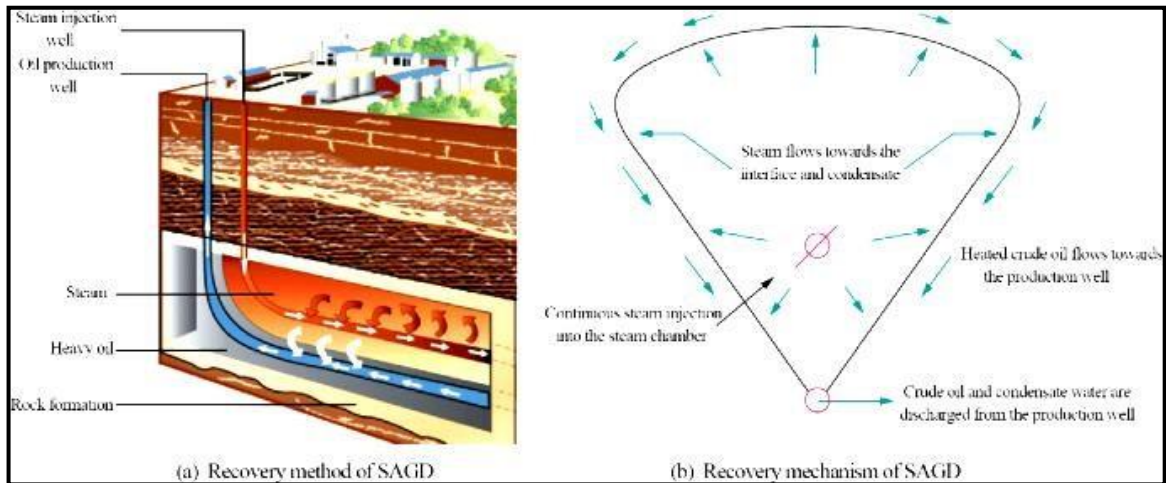


Figure II.11: Recovery process and mechanism of SAGD [94].

II-4 Relationship between oil recovery and pore geometry

The interplay between pore geometry and oil recovery in porous media reservoirs can be established by grasping how pore-scale structures interact with fluid dynamics and how each aspect of pore geometry particularly influences oil recovery, either by reducing it or increasing it, as follows:

II-4-1 Pores size

Larger pores provide less resistance to fluid flow, resulting in higher fluid mobility and permeability, leading to higher initial recovery rates. However, narrow pore sizes can cause bypassed areas, ineffective sweeping, and reduced recovery efficiency. By modulating pore throat accessibility, capillary pressure, and fluid storage capacity [95].

II-4-2 Pores shape

The shape of pores affects the tortuosity of fluid flow paths. Surface area-to-volume ratios and capillary forces as Uniform and well-defined pores have better fluid sweep efficiency, while complex, irregular, or tortuous pores may require more sophisticated recovery methods because they can impede fluid flow and increase flow resistance [96].

II-4-3 Pores connectivity

Fluid movement, migration, and efficient exchange between pores are made possible by the high pore connectivity, which promotes uniform fluid distribution and reservoir sweep. Throughout the primary and secondary recovery phases, improved overall recovery factors and a reduced chance of bypassed areas are a result of improved connectivity [97].

II-4-4-Pores tortuosity

Tortuous pore structures result in lengthening the effective path for fluid flow, thus lowering flow rates and performing less permeability by reducing sweep efficiency and

impeding fluid motion in complex pore networks. However, moderate tortuosity can enhance oil recovery by creating additional contact points between injected fluid and trapped hydrocarbons, promoting effective fluid-rock interaction and oil displacement, increasing surface area, and enhancing capillary forces [98].

II-4-5-Pore Size Distribution

The distribution of pore sizes affects a reservoir's ability to store and access fluids, with wide dispersion leading to uneven fluid saturation. Well-defined and narrow-pore-size reservoirs have higher recovery efficiency and uniform distribution, while extensive distributions may cause unequal fluid saturation [99].

II-4-6-Heterogeneity

The variations create preferential flow paths and encourage fluid movement, leading to a more effective sweep of hydrocarbons within the reservoir. Channels formed by high-permeability zones in heterogeneous reservoirs facilitate the movement of injected fluids, such as water or gas, enabling them to access and displace oil from previously unreachable areas. Additionally, it can lead to the creation of natural fractures or faults, which act as conduits for fluid flow and increase connectivity.

Conversely, it poses difficulties for fluid sweep and recovery because it might cause some areas to flow more preferentially than others. As fluid channeling, bypassing of oil-rich zones, and the formation of stagnant regions. Channels or fractures may act as shortcuts for injected fluids, resulting in premature breakthrough and consequently decreasing sweep efficiency as large volumes of fluid bypass oil-rich zones without adequately displacing hydrocarbons [96].

II-5 Pore-Scale phenomena in fluid flow

II-5-1 Snap-Off phenomenon

Snap-off occurs when a wetting fluid (water) displaces a non-wetting fluid (oil), trapping it in isolated pockets or ganglia within pore spaces. The non-wetting phase detaches from the wetting phase as a result of the cooperation of capillary and viscous forces. This process is influenced by the geometry of the trapped oil pockets, with narrow pores or throats showing more noticeable snap-off (Figure II.12), where capillary forces predominate due to higher capillary pressures and the curvature of fluid interfaces. Primary recovery results in lower sweep efficiency, leaving residual oil in the reservoir. In secondary recovery methods, snap-off can enhance recovery rates by mobilizing stored oil and thus displacing it [100].



Figure II.12: Snap-off diagram in a pore groove: The solid is black, the water is grey and the gas is white [101].

II-5-2 Jamin effect phenomena

The resistance that the presence of bubbles creates to liquid flow in capillaries is known as the Jamin effect. The oil's movement toward a production well is found to be delayed by the Jamin effect (Figure II.13) [102].

It occurs due to the curvature of the fluid-fluid interface at the pore scale, leading to variations in capillary pressure within the pore spaces that alter the fluid distribution and flow characteristics.

Significant Curvature in pores can raise capillary pressures, restrict fluid flow, and trap fluids, reducing rock permeability. Following displacement procedures, the trapped oil zones cannot be accessed, resulting in lower sweep efficiency and reservoir oil recovery. Secondary recovery methods, like water flooding, affect displacement efficiency by changing the fluid distribution and decreasing mobility. The Jamin effect is crucial for maximizing fluid displacement and oil recovery rates in tertiary recovery. Engineers can improve sweep efficiency by adjusting injection rates, fluid properties, and reservoir conditions to mobilize trapped oil [103], [104].

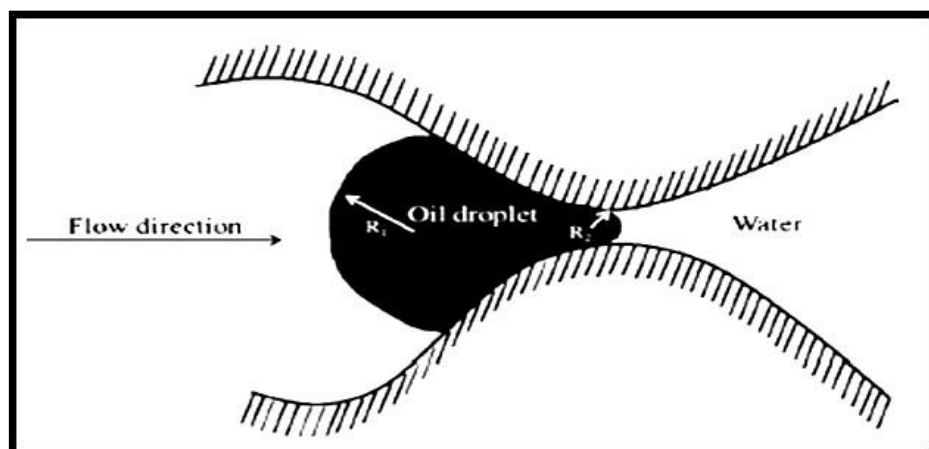


Figure II.13: Trapped capillary drop: Jamin effect [105].

II-5-3 Bypass phenomena

Bypass phenomena occur when a fluid phase, like gas or oil, is not effectively recovered or displaced during fluid injection procedures in porous materials. This occurs due to the preferred movement of the displacing fluid phase and the uneven distribution of fluid flow paths due to heterogeneous pore structures, causing parts of the reservoir to be bypassed or insufficiently swept. Because of ineffective fluid sweep during primary recovery, bypassed zones may contain sizable volumes of trapped oil, which would reduce recovery factors. Secondary recovery strategies aim to increase fluid sweep efficiency. Improved oil recovery techniques aim to bypass oil by altering fluid characteristics to release trapped hydrocarbons [29].

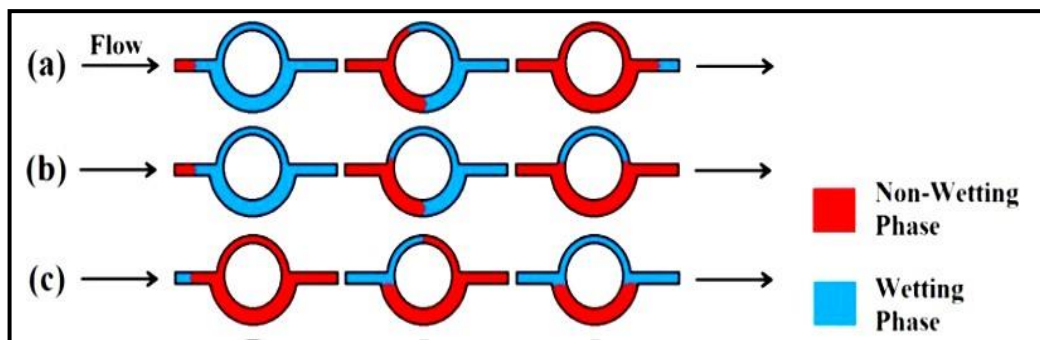


Figure II.14: Bypassing phenomena illustration, a) Drainage Process, No Trapping, b) Drainage Process, Bypassing in Smaller Throat, c) Imbibitions Process, Bypassing in Larger Throat [29].

II-5 -4 Water block phenomena

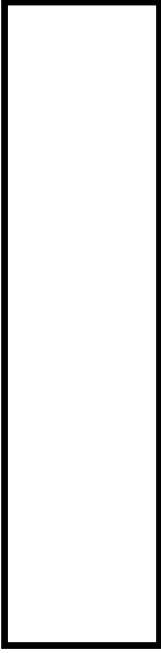
A water block occurs when water infiltrates the area surrounding the well during a drilling operation in a reservoir, leading to the formation of water barriers or blockages within the pore spaces. Where the relative permeability is decreased [106].

Capillary pressures in pores with irregular shapes and smaller diameters increase water blockage, preventing oil displacement. Interconnected pores facilitate water blockage propagation. Reducing sweep efficiency during primary recovery and forming bypassed zones for trapped hydrocarbons. In secondary recovery methods, water blockages may reduce oil recovery and cause inefficient sweeping. While severe obstructions in reservoirs can hinder enhanced oil recovery techniques, necessitating additional measures to improve recovery rates [107].

Conclusion

In conclusion, the study of dynamic properties in porous media represents a cornerstone in the field of reservoir engineering and hydrocarbon recovery. Throughout this

chapter, we have explored the multifaceted nature of reservoir permeability, measurement methodologies, and advanced recovery strategies. By delving into the intricate relationship between pore geometry and oil recovery, we have gained insights into the complex interplay of factors influencing fluid flow dynamics. Furthermore, the examination of fluid preferential flow pathways and its several phenomenon's' have highlighted the importance of understanding and mitigating potential flow barriers to optimize recovery efforts. As we continue to advance our understanding of dynamic fluid behavior, we are poised to unlock new avenues for enhancing hydrocarbon recovery and maximizing reservoir performance. This information's establish the groundwork for experimental procedures aiming at understanding the influence of pore geometry on the relative permeability of water and oil, as well as the effectiveness of oil recovery, which are explained in the next chapter.



*Conclusion and
recommandations*

Conclusion and recommendations

The purpose of this study was to simulate and characterize the displacement of two-phase (water-oil) flow in porous media and to explore the influence of pore geometry on oil recovery. The study aimed to answer several critical questions:

- How does pore geometry affect the permeability and preferential flow of water and oil?
- What is the impact of clay content on fluid pathways and oil recovery?
- How effective are different heat-based oil recovery techniques?

The literature review underscored the importance of understanding fluid flow dynamics in heterogeneous porous media, the role of pore structure in oil recovery, and the utilization of advanced visualization techniques to observe these processes in real-time. The study employed a methodology that included measurements of porosity, relative permeabilities, saturation, and incremental oil rates using powdered micromodels with various pore sizes. Real-time visual observations were conducted using a PVC-mesofluidic system to analyze fluid interactions at the pore scale.

Key findings of the study included that:

1. Larger pores provided less resistance to fluid flow, resulting in higher permeability.
2. Clay content significantly impacted fluid pathways, reducing diesel permeability more than water permeability.
3. Heat-based oil recovery methods showed varied efficacy depending on pore geometry.
4. From the findings, several significant conclusions can be drawn:
5. Impact of Pore Geometry: The study confirmed that pore size and distribution significantly influence fluid flow dynamics. Larger pores enhance oil recovery by providing continuous pathways for fluid flow, whereas smaller pores can trap water and impede overall flow. This insight underscores the importance of characterizing pore structures in reservoir rocks to optimize oil recovery strategies.
6. Effect of Clay Content: The presence of clay within the porous media was found to alter fluid pathways, favoring water flow due to its hydrophilic nature while restricting oil flow. This phenomenon is attributed to the increased capillary forces in clay-rich regions, which makes it more challenging for oil to displace water. Therefore, clay content must be a crucial consideration in reservoir management and the design of recovery methods.

7. Effectiveness of Heat-Based Recovery Techniques: Heat-based recovery methods, such as steam injection, were observed to improve oil displacement efficiency. However, their effectiveness was highly dependent on the specific pore structure of the reservoir. This finding suggests that the success of thermal recovery methods can vary widely and should be tailored to the reservoir's geological characteristics.
8. The conclusions of this study are consistent with previous research that highlights the significant role of pore geometry and mineral content in influencing hydrocarbon recovery. The finding that larger pores facilitate better oil flow aligns with existing theories on permeability and fluid dynamics in porous media. Additionally, the observed impact of clay content on restricting oil flow due to enhanced capillary forces reinforces the importance of understanding the mineralogical composition of reservoirs.

9. Advanced visualization techniques used in this study provided unprecedented insights into fluid interactions at the micro-scale. These techniques allowed for more accurate predictions of recovery efficiency and demonstrated the complex interplay between pore structure and fluid dynamics. The real-time observations enabled a deeper understanding of how different recovery methods interact with the reservoir rock, which is considered a base for developing more effective extraction techniques.

Based on the study's findings, several recommendations can be made for practitioners in reservoir engineering:

1. Tailored Recovery Strategies: Develop recovery techniques that are customized to the specific pore structures and mineral content of the reservoir.
2. This approach will ensure that the chosen method aligns with the reservoir's unique characteristics, thereby maximizing oil recovery.
3. Advanced Visualization Techniques: Employ real-time visualization methods to monitor fluid flow dynamics and adjust recovery strategies accordingly. This will provide continuous feedback and allow for the optimization of recovery processes in response to observed changes.
4. Clay Management: Implement strategies to mitigate the impact of clay on oil recovery. Chemical treatments to alter wettability or mechanical methods to modify pore structures could be effective in enhancing oil flow in clay-rich reservoirs.
5. Optimization of Heat-Based Techniques: Conduct preliminary assessments of pore geometry before applying heat-based recovery methods. This will help predict their efficacy and allow for the optimization of thermal recovery processes.

Suggestions for Further Research

Future research should focus on:

Long-Term Field Studies: Conducting extended field studies to validate laboratory findings and assess the long-term effectiveness of tailored recovery strategies. These studies will provide practical insights and help refine recovery techniques for real-world applications.

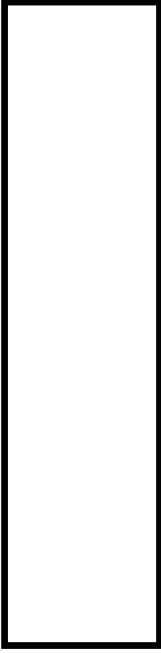
Advanced Materials and Nanotechnology: Exploring the use of advanced materials and nanotechnology to modify pore structures and enhance fluid flow. Innovations in material science could lead to new methods for improving oil recovery in challenging reservoir conditions.

Environmental Impact Assessment: Evaluating the environmental impact of different recovery techniques and developing more sustainable methods. This is crucial for ensuring that oil recovery processes do not adversely affect the environment.

In conclusion, this study has provided valuable insights into the influence of pore geometry and mineral content on fluid flow dynamics and oil recovery. By leveraging advanced visualization techniques and tailored recovery strategies, it is possible to enhance hydrocarbon extraction and optimize reservoir performance. The findings emphasize the critical importance of characterizing reservoir heterogeneity and developing customized recovery methods that account for the unique geological features of each reservoir.

The research contributes to the broader understanding of how micro-scale interactions between fluids and pore structures influence macro-scale recovery outcomes. It underscores the need for a multidisciplinary approach that integrates geology, fluid dynamics, and engineering to tackle the complex challenges of oil recovery.

Future research and practical applications should build on these findings to develop more efficient, sustainable, and adaptable oil recovery techniques. This will not only improve the economic viability of hydrocarbon extraction but also ensure that it is conducted in an environmentally responsible manner.



Bibliographic references

Bibliographic references

- [01] Hewitt, C. H.: "How Geology Can Help Engineer Your Reservoirs», Oil and Gas J. (Nov. 14, 1966) 64,171.
- [02] Hewitt, C. H. and Morgan, J. T.: "The Fry in Situ Combustion Test- Reservoir Characteristics", J. Pet. Tech. (March, 1965) 337-342.
- [03] Wayhan, D. A and McCaleb, J. A : "Elk Basin Madison Heterogeneity-Its Influence on Performance", J. Pet. Tech. (Feb., 1969) 153-159
- [04] Zhong, R., Yao, L., Zhao, Y., Zhao, D., & Li, Z. (2022). Analysis of factors affecting thermal recovery of porous media in heavy oil reservoir. Journal of Physics. Conference Series,2208(1), 012005. <https://doi.org/10.1088/1742-6596/2208/1/012005>
- [05] Javaran, E. J., Nassab, S. G., & Jafari, S. (2010). Thermal analysis of a 2-D heat recovery sytem using porous media including lattice Boltzmann simulation of fluid flow. International Journal of Thermal Sciences, 49(6), 1031–1041. <https://doi.org/10.1016/j.ijthermalsci.2009.12.004>
- [06] Feder, J., Flekkøy, E. G., & Hansen, A. (2022). *Physics of Flow in Porous Media*.
- [07] Bejan, A., Dincer, I., Lorente, S., Miguel, A. F., & Reis, A. H. (2004). Porous and Complex Flow Structures in Modern Technologies. <https://doi.org/10.1007/978-1-4757-4221-3>
- [08] Metzger, T., Irawan, A., & Tsotsas, E. (2007, February 12). Isothermal Drying of Pore Networks: Influence of Friction for Different Pore Structures. *Drying Technology*, 25(1), 49 <https://doi.org/10.1080/07373930601152640>
- [9] Coussot, P. (2014, June 17). *Rheophysics*. Springer. http://books.google.ie/books?id=De8pBAAAQBAJ&pg=PR4&dq=978-3-319-06148-1&hl=&cd=1&source=gbs_api
- [10] Bear, J. (2013, February 26). *Dynamics of Fluids in Porous Media*. Courier Corporation. http://books.google.ie/books?id=fBMeVSZ_3u8C&printsec=frontcover&dq=Bear,+J.,+Dynamics+Of+Fluids+In+Porous+Media,+DOVER+PUBLICATIONS,+INC,+New+York,+756+pages,+1972.&hl=&cd=1&source=gbs_api
- [11] M. Bonnet et A. Lallemand-Barres (1970). Mesure de la vitesse d'écoulement en milieu saturé par les méthodes de traçage. Etude documentaire, bureau de recherches géologiques et minières. B.P.6009-45 Orléans (02). Décembre 1970.
- [12] "Mécanique des Fluides" by Marc Fermigier, dated February 7, 2024, discussing fluid mechanics and various related topics

Bibliographic references

- [13] Franck Laurel Nono Nguendjio. Caractérisation polyphasique de la zone de transition, dans un réservoir pétrolier carbonaté. Mécanique [physics.med-ph]. Ecole nationale supérieure d'arts et métiers - ENSAM, 2014. Français. NNT: 2014ENAM0012.
- [14] Yra A. Dispersion active en milieux poreux hétérogènes contaminés par des produits hydrocarbonés. Thèse à l'université de Bordeaux1, 2006.
- [15] Nguendjio, F. L. N. (2014, April 30). Caractérisation polyphasique de la zone de transition dans un réservoir pétrolier carbonaté. <https://www.theses.fr/2014ENAM0012.pdf>
- [16] Aminpour, M. (2018). Pore-scale behaviors of the Darcy flow in static and dynamic porous
- [17] Kahyarian, A., Achour, M., & Nešić, S. (2017, January 1). CO₂ corrosion of mild steel. Elsevier eBooks. <https://doi.org/10.1016/b978-0-08-101105-8.00007-3>
- [18] <https://www.araboil-naturalgas.com>. Visited 05/05/2024 1:08 am
- [19] <https://www.thermopedia.com/content/4/>. Visited 05/05/2024 01:19 am
- [20] Bird, R. B., Lightfoot, E. N., & Stewart, W. E. (2002, January 1). Transport Phenomena. John Wiley & Sons. http://books.google.ie/books?id=wYnRQwAACAAJ&dq=Transport+Phenomena+by+Bird,+Stewart,+and+Lightfoot.&hl=&cd=2&source=gbs_api
- [21] Crowe, C. T., Schwarzkopf, J. D., Sommerfeld, M., & Tsuji, Y. (2011, August 26). Multiphase Flows with Droplets and Particles, Second Edition. CRC Press. http://books.google.ie/books?id=XewhTKFFv4EC&printsec=frontcover&dq=Multiphase+Flows+with+Droplets+and+Particles%22+by+Clayton+T.+Crowe,+et+al.&hl=&cd=1&source=gbs_api
- [22] Michaelides, E., Crowe, C. T., & Schwarzkopf, J. D. (2016, October 26). Multiphase Flow Handbook. CRC Press. http://books.google.ie/books?id=xhwNDgAAQBAJ&printsec=frontcover&dq=Multiphase+Flow+Handbook&hl=&cd=1&source=gbs_api
- [23] Brill, J. P., & Beggs, H. D. (1991, January 1). Two-phase Flow in Pipes. http://books.google.ie/books?id=PNPbnQEACAAJ&dq=Two-Phase+Flow+in+Pipes%22+by+Jean-Pierre+Delplanque&hl=&cd=4&source=gbs_api
- [24] Cholet, H. (2008, January 1). Well Production Practical Handbook. http://books.google.ie/books?id=8-z9xwEACAAJ&dq=Well+Production+Practical+Handbook+Par+Henri+Cholet+%C2%B7+2008&hl=&cd=1&source=gbs_api

Bibliographic references

- [25] NargesDashtbeshbadounak. Upscaling multiphase flows in heterogeneous porous media and its application to EOR. Applied geology. Sorbonne University, 2021. English. NNT: 2021SORUS084. Tel-03615453
- [26] Chen, Z., Huan, G., & Ma, Y. (2006, April 1). Computational Methods for Multiphase Flows in Porous Media. SIAM. http://books.google.ie/books?id=qhQY8YlnDW8C&printsec=frontcover&dq=Computational+Methods+%0D%0Afor+Multiphase+Flows+%0D%0Ain+Porous+Media&hl=&cd=1&source=gbs_api
- [27] Negara, A. (2015, August 24). Multiphase Flow Simulation with Gravity Effect in Anisotropic Porous Media using Multipoint Flux Approximation. Kaust. https://www.academia.edu/12332538/Multiphase_Flow_Simulation_with_Gravity_Effect_in_Anisotropic_Porous_Media_using_Multipoint_Flux_Approximation
- [28] Ahammad, M. J., & Alam, J. M. (2017, April 30). A numerical study of two-phase miscible flow through porous media with a Lagrangian model. The Journal of Computational Multiphase Flows. <https://doi.org/10.1177/1757482x17701791>
- [29] Bob, B. (2016, October 25). Fundamentals of Fluid Flow in Porous Media. Special Core Analysis & EOR Laboratory | PERM Inc. <https://perminc.com/resources/fundamentals-of-fluid-flow-in-porous-media/chapter-2-the-porous-medium/>
- [30] Zhou, Y., Zhang, G., & Liu, J. (2022, February 17). Modeling Method to Characterize the Pore Structure of Fractured Tight Reservoirs. Applied Sciences. <https://doi.org/10.3390/app12042078>
- [31] FOUCAULT, Raoult. FOUCAULT A., RAOULT J. F.–Dictionnaire de géologie. Éditions Masson, Paris, 1992
- [32] WALSH, J. B. et BRACE, W. F. Cracks and pores in rocks. In: 1st ISRM Congress. OnePetro, 1966
- [33] BERNABE, Y. Pore geometry and pressure dependence of the transport properties in sandstones. Geophysics, 1991, vol. 56, no 4, p. 436-446.
- [34] FREDRICH, J. T., GREAVES, K. H., et MARTIN, J. W. Pore geometry and transport properties of Fontainebleau sandstone. In: International journal of rock mechanics and mining sciences & geomechanics abstracts. Pergamon, 1993. p. 691-697
- [35] GUEGUEN, Yves, DAVID, Christian, et DAROT, Michel. Models and time constants for permeability evolution. Geophysical Research Letters, 1986, vol. 13, no 5, p. 460-463.

Bibliographic references

- [36] GUÉGUEN, Yves et PALCIAUSKAS, Victor. Introduction à la physique des roches. Paris: Hermann, 1992.
- [37] ZHU, Wenlu, DAVID, Christian, et WONG, Teng-fong. Network modeling of permeability evolution during cementation and hot isostatic pressing. *Journal of Geophysical Research: Solid Earth*, 1995, vol. 100, no B8, p. 15451-15464.
- [38] LARIVE, Elodie. Experimental study of very low permeability rocks using a high accuracy permeameter; Etude experimentale des roches a tresfaiblepermeabilite par la mise en oeuvre d'un permeametre de precision. 2002.
- [39] KEANEY, Gemma Maria Jacinta. Experimental study of the evolution of permeability in rocks under simulated crustal stress conditions. University of London, University College London (United Kingdom), 2000.
- [40] Hutin, A. (2022, March 28). Porous media in reservoir engineering: Introduction. ResearchGate. <https://doi.org/10.5281/zenodo.6391053>
- [41] Klinkenberg, L.J.. "Pore Size Distribution of Porous Media and Displacement Experiments with Miscible Liquids." *J Pet Technol* 9 (1957)
- [42] Rahaman, M. N. (2010, January 1). Kinetics and mechanisms of densification. Elsevier eBooks. <https://doi.org/10.1533/9781845699949.1.33>
- [43] Selvadurai, A. P. S., & Suvorov, A. P. (2020, November 3). The influence of the pore shape on the bulk modulus and the Biot coefficient of fluid-saturated porous rocks. *Scientific Reports*. <https://doi.org/10.1038/s41598-020-75979-6>
- [44] Clennell, M. B. (1997, January). Tortuosity: a guide through the maze. *Geological Society, London, Special Publications*, 122(1), 299–344. <https://doi.org/10.1144/gsl.sp.1997.122.01.18>
- [45] Crain, E. R. (1986, January 1). *The Log Analysis Handbook: Quantitative log analysis methods*. http://books.google.ie/books?id=bIIZAQAIAAJ&q=Crain%27s+Petrophysical+Handbook&dq=Crain%27s+Petrophysical+Handbook&hl=&cd=1&source=gbs_api
- [46] Total. LE PROCESS: INTRODUCTION AU GISEMENT. SUPPORT DE FORMATION Cours EXP-PR-PR015 Révision 0.1. 28/04/2007
- [47] CPH | Chapter And Topic Index. (n.d.). <https://spec2000.net/index.htm>
- [48] ElGendy, A. M. (2016, January 26). Determination of irreducible water saturation Shams. https://www.academia.edu/20853971/Determination_of_Irreducible_Water_Saturation?t

Bibliographic references

- [49] Ahmed, Tarek, McKinney, Paul, et al., *Advanced Reservoir Engineering* Elsevier, 2011. TN871 A337 2000, p. 190.
- [50] <https://www.collegesidekick.com/study-docs/696842> . Visited
- [51] GIBBS, J. Willard. *The Collected Works of J. Willard Gibbs, Ph. D., LL. D. (No Title)*, 1931.
- [52] Smith, J. E., & Zhang, F. (2001, March 1). Determining effective interfacial tension and predicting finger spacing for DNAPL penetration into water-saturated porous media. *Journal of Contaminant Hydrology*.
- [53] Interfacial Tension - FasterCapital. (n.d.). FasterCapital. <https://fastercapital.com/keyword/interfacial-tension.html>
- [54] Fitch, J. (2019, August 29). The Surface Tension Test - Is It Worth Resurrecting? *Machinery Lubrication*. <https://www.machinerylubrication.com/Read/376/surface-tension-test>
- [55] FLUID FLOW IN POROUS MEDIA by Zoltán E. HEINEMANN Professor for Reservoir Engineering Leoben, October 2005
- [56] (PDF) Experimental reservoir engineering laboratory workbook. (n.d.). ResearchGate. https://www.researchgate.net/publication/286042184_Experimental_reservoir_engineering_laboratory_workbook/figures?lo=1
- [57] LeonhardGanzer. (2017, September 11). *Enhanced Oil Recovery Fundamentals*
- [58] Thomas Young. An essay on the cohesion of fluids. *Philosophical Transactions of the Royal Society of London*, 95:65-87, 1805
- [59] Eshiet, K. I. I. I., &GMoghanloo, R. (2022, November 2). *Emerging Technologies in Hydraulic Fracturing and Gas Flow Modelling*. BoD – Books on Demand
- [60] ANDERSON, William G. Wettability literature survey-part 4: Effects of wettability on capillary pressure. *Journal of petroleum technology*, 1987, vol. 39, no 10, p. 1283-1300
- [61] Wang, Y., Xu, H., Yu, W., Bai, B., Song, X., & Zhang, J. (2011, December). Surfactant induced reservoir wettability alteration: Recent theoretical and experimental advances in enhanced oil recovery. *Petroleum Science*, 8(4), 463–476. <https://doi.org/10.1007/s12182-011-0164-7>
- [62] Brown, R.J.S and Fatt, I., Measurements of Fractional Wettability of Oil Field Rocks by the Nuclear Magnetic Relaxation Method. *Transactions,AIME*. 1956.207, 262-264
- [63] Zahoor, M. K., Derahman, M. N., & Yunan, M. H. (2011, June 24). WAG PROCESS DESIGN – AN UPDATED REVIEW. *Brazilian Journal of Petroleum and Gas*, 5(2), 109–121. <https://doi.org/10.5419/bjpg2011-0012>

Bibliographic references

- [64] Alhammadi, A. M., AlRatrouf, A., Singh, K., Bijeljic, B., & Blunt, M. J. (2017, September 7). In situ characterization of mixed-wettability in a reservoir rock at subsurface conditions. *Scientific Reports*, 7(1). <https://doi.org/10.1038/s41598-017-10992-w>
- [65] EmamiMeybodi, H., Kharrat, R., & NasehiAraghi, M. (2011, August). Experimental studying of pore morphology and wettability effects on microscopic and macroscopic displacement efficiency of polymer flooding. *Journal of Petroleum Science and Engineering*, 78(2), 347–363. <https://doi.org/10.1016/j.petrol.2011.07.004>
- [66] Donaldson, E. C., & Tiab, D. (2004, January 24). *Petrophysics*. Elsevier. http://books.google.ie/books?id=pGb6jaa5IVYC&pg=PR4&dq=0-7506-7711-2&hl=&cd=1&source=gbs_
- [67] Cossé, R. (1988, January 1). *Techniques d'exploitation pétrolière*. Editions TECHNIP. http://books.google.ie/books?id=r036L-y9eTYC&pg=PA3&dq=Le+gise%3Bet+rene+cosse&hl=&cd=2&source=gbs_api
- [68] (2022, March 30). *Les milieux poreux en ingénierie de réservoir : Perméabilité*. Zenodo. <https://doi.org/10.5281/zenodo.6399277>
- [69] Chilingarian, G. V. "Relationship between Porosity, Permeability and Grain Size Distribution of Sands and Sandstones." In: Van Straaten, J. U.(Ed.), *Deltaic and Shallow Marine Deposits*. Elsevier Science Pubi. Co.,New York, Amsterdam, 1963, pp. 71-75.
- [70] Clark, N. J. *Elements of Petroleum Reservoirs*, revised ed. Society of Petroleum Engineers, Dallas, TX, Henry L. Doherty Series, 1969, pp. 19-30.
- [71] Choquette, P. W. and Pray, L. C. "Geologic Nomenclature and Classification of Porosity in Sedimentary Carbonates." *Am. Assoc. Petrol. Geol. (AAPG) Bull.*, Vol. 54, 1970, pp. 207-250.
- [72] BUCKLEY, Se E. et LEVERETT, M.Ci. Mechanism of fluid displacement in sands. *Transactions of the AIME*. 1942, vol. 146, no 01, p. 107-116
- [73] WELGE, Henry J. A simplified method for computing oil recovery by gas or water drive. *Journal of Petroleum Technology*, 1952, vol. 4, no 04, p. 91-98
- [74] JOHNSON, E. F., BOSSLER, D. P., et BOSSLER, VO Naumann. Calculation of relative permeability from displacement experiments. *Transactions of the AIME*, 1959, vol. 216, no 01, p. 370-372
- [75] J P Bloomfield (May 1993) «Laboratory determination of wettability, capillary pressure curves, pore entry pressure and relative permeabilities in immiscible phase-brine systems». Technical Report: WD/93/24R, NERC copyright 1993 keyworth, Nottinghamshire. British Geological Survey 1993, p.20-21-22.

Bibliographic references

- [76] Adjie, B. (2016, May 25). Formation Evaluation MSc Course Notes.
- [77] ABRAMS, Albert. The influence of fluid viscosity, interfacial tension, and flow velocity on residual oil saturation left by waterflood. Society of Petroleum engineering journal
- [78] Fulcher, R.A., Ertekin, Turgay, and C.D. Stahl. "Effect of Capillary Number and Its Constituents on Two-Phase Relative Permeability Curves." J Pet Technol 37 (1985): 249–260. doi: <https://doi.org/10.2118/12170-PA>
- [79] Wang, S., Feng, Q., & Han, X. (2013, December 30). A Hybrid Analytical/Numerical Model for the Characterization of Preferential Flow Path with Non-Darcy Flow. PloS One. <https://doi.org/10.1371/journal.pone.0083536>
- [80] Engström, E., Thunvik, R., Kulabako, R., & Balfors, B. (2014, October 21). Water Transport, Retention, and Survival of Escherichiacoli in Unsaturated Porous Media: A Comprehensive Review of Processes, Models, and Factors. Critical Reviews in Environmental Science and Technology, 45(1), 1–100. <https://doi.org/10.1080/10643389.2013.828363>
- [81] Parra, J. E., Samaniego-V, F., & Lake, L. W. (2023, March 27). Application of the Producer-Based Capacitance Resistance Model to Undersaturated Oil Reservoirs in Primary Recovery. Spe Journal. <https://doi.org/10.2118/214678-pa>
- [82] Fernando, J. (2022, July 18). Primary Recovery: What it Means, How it Works. Investopedia. <https://www.investopedia.com/terms/p/primary-recovery.asp>
- [83] primary_recovery. (n.d.). https://glossary.slb.com/terms/p/primary_recovery
- [84] Primary Recovery. (n.d.). <https://www.ideo.columbia.edu/users/menke/ENERGY/CH07/img16.html> 05/04/2024 00:30
- [85] Ezekwe, N. (n.d.). Petroleum Reservoir Engineering Practice. O'Reilly Online Learning. <https://www.oreilly.com/library/view/petroleum-reservoir-engineering/9780132485210/ch16.html>
- [86] Secondary recovery. (n.d.). Encyclopedia Britannica. <https://www.britannica.com/technology/secondary-recovery>
- [87] Secondary Recovery Technique | Encyclopedia.com. (n.d.). <https://www.encyclopedia.com/environment/encyclopedias-almanacs-transcripts-and-maps/secondary-recovery-technique>

Bibliographic references

- [88] Ganat, T. (2019, December 18). Pumping System of Heavy Oil Production. Processing of Heavy Crude Oils - Challenges and Opportunities. <https://doi.org/10.5772/intechopen.87077>
- [89] Muggeridge, A., Cockin, A., Webb, K. J., Frampton, H., Collins, I., Moulds, T., & Salino, P. (2014, January 13). Recovery rates, enhanced oil recovery and technological limits. *Philosophical Transactions of the Royal Society A*. <https://doi.org/10.1098/rsta.2012.0320>
- [90] Enhanced Oil Recovery. (n.d.). Energy.gov. <https://www.energy.gov/fecm/enhanced-oil-recovery> 04/04/2024 18:22
- [91] Lee, K. S., Kwon, T., Park, T., & Jeong, M. S. (2020, January 1). Microbiology and Microbial Products for Enhanced Oil Recovery. Elsevier eBooks. <https://doi.org/10.1016/b978-0-12-819983-1.00002-8>
- [92] Fernando, J. (2024, March 21). Tertiary Recovery: What it Means, how it Works. Investopedia. <https://www.investopedia.com/terms/t/tertiary-recovery.asp>
- [93] Mokheimer, E. M. A., Hamdy, M., Abubakar, Z., Shakeel, M. R., Habib, M. A., & Mahmoud, M. (2018, September 14). A Comprehensive Review of Thermal Enhanced Oil Recovery: Techniques Evaluation. *Journal of Energy Resources Technology*, 141(3). <https://doi.org/10.1115/1.4041096>
- [94] Dai, C., You, Q., Zhao, M., Zhao, G., Zhao, F. (2023). Thermal Oil Recovery. In: *Principles of Enhanced Oil Recovery*. Springer, Singapore. https://doi.org/10.1007/978-981-99-0193-7_10
- [95] Liu, J.; Li, H.; Xu, J.; Liu, S.; Liu, R.; Hou, L.; Tan, Q. Exploring the Unique Characteristics of High-Pore-Volume Waterflooding and Enhanced Oil Recovery Mechanisms in Offshore. *J. Mar. Sci. Eng.* 2023, 11, 1296. <https://doi.org/10.3390/jmse11071296>
- [96] Investigation of pore geometry influence on fluid flow in heterogeneous porous media. *Petroleum Research*, 2023, 8(2), 100689. <https://doi.org/10.1016/j.ptlrs.2023.100689>
- [97] Skills, G. (n.d.). Porosity. <https://www.geo-skill.com/2021/08/porosity.html>
- [98] Guo, P. (2012, July 25). Dependency of Tortuosity and Permeability of Porous Media on Directional Distribution of Pore Voids. *Transport in Porous Media*, 95(2), 285–303. <https://doi.org/10.1007/s11242-012-0043-8>
- [99] Xu, Y., Li, Q., & King, H.E, Modeling Oil Recovery for Mixed Macro- and Micro-Pore Carbonate Grainstones. 7, 9780 (2017). <https://doi.org/10.1038/s41598-017-09507-4>
- [100] Li, G., & Yao, J. (2023, November 17). Snap-Off during Imbibition in Porous Media:

Bibliographic references

Mechanisms, Influencing Factors, and Impacts. Eng. <https://doi.org/10.3390/eng4040163>

[101] Liu, J., & Yi, L. (2018, July 14). *Liquid Metal Biomaterials*. Springer.

http://books.google.ie/books?id=VQ9kDwAAQBAJ&printsec=frontcover&dq=ROSSEN,+William+R.+Snapoff+in+constricted+tubes+and+porous+media.+Colloids+and+Surfaces+A:+Physicochemical+and+Engineering+Aspects,+2000,+vol.+166,+no+1-3,+p.+101-107.&hl=&cd=1&source=gbs_api

[102] Randall Wright (2). (1933). Jamin Effect in Oil Production. *AAPG Bulletin*, 17. <https://doi.org/10.1306/3d932bdc-16b1-11d7-8645000102c1865d>

[103] Liu, S., Dou, X., Zeng, Q., & Liu, J. (2021, January). Critical parameters of the Jamin effect in a capillary tube with a contracted cross section. *Journal of Petroleum Science and Engineering*, 196, 107635. <https://doi.org/10.1016/j.petrol.2020.107635>

[104] Zhao, J., Yao, G., & Wen, D. (2019, October 1). Pore-scale simulation of water/oil displacement in a water-wet channel. *Frontiers of Chemical Science and Engineering*, 13(4), 803–814. <https://doi.org/10.1007/s11705-019-1835-y>

[105] Moradi, M., Kazempour, M., French, J. T., & Alvarado, V. (2014, November). Dynamic flow response of crude oil-in-water emulsion during flow through porous media. *Fuel*, 135, 38–45. <https://doi.org/10.1016/j.fuel.2014.06.025>

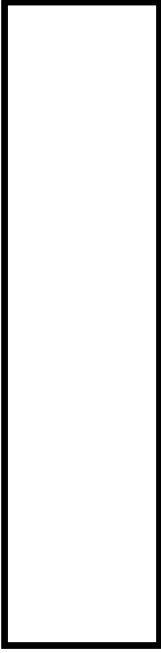
[106] Jagannathan Mahadevan and Mukul M. Sharma., 2003. Clean-up of Water Blocks in Low Permeability Formations. Paper SPE 84216 presented at the SPE Annual Technical Conference and Exhibition, Denver, 5–8 October (2003) <http://dx.doi.org/10.2118/84216-MS>.

[107] Shao, C., Yang, Z., Zhou, G., & Lu, G. (2010, August 3). Pore network modeling of water block in low permeability reservoirs. *Petroleum Science*, 7(3), 362–366. <https://doi.org/10.1007/s12182-010-0078-9>

[108] Rezaei, M., Seuntjens, P., Joris, I., Boënné, W., Van Hoey, S., Campling, P., & Cornelis, W. M. (2016, January 29). Sensitivity of water stress in a two-layered sandy grassland soil to variations in groundwater depth and soil hydraulic parameters. *Hydrology and Earth System Sciences*, 20(1), 487–503. <https://doi.org/10.5194/hess-20-487-2016>

[109] Bergane, C., & Hammadi, L. (2020, September 27). Impact of organophilic clay on rheological properties of gasoil-based drilling muds. *Journal of Petroleum Exploration and Production Technology*, 10(8), 3533–3540. <https://doi.org/10.1007/s13202-020-01008-x>

[110] Clay | Definition, Formation, Properties, Uses, & Facts. (1998, July 20). *Encyclopedia Britannica*. <https://www.britannica.com/science/clay-geology>

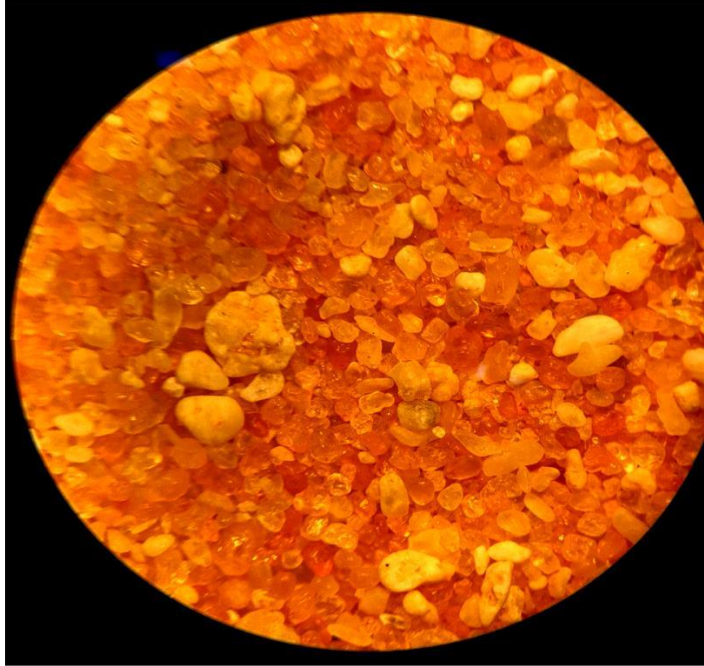


Appendix

Appendix

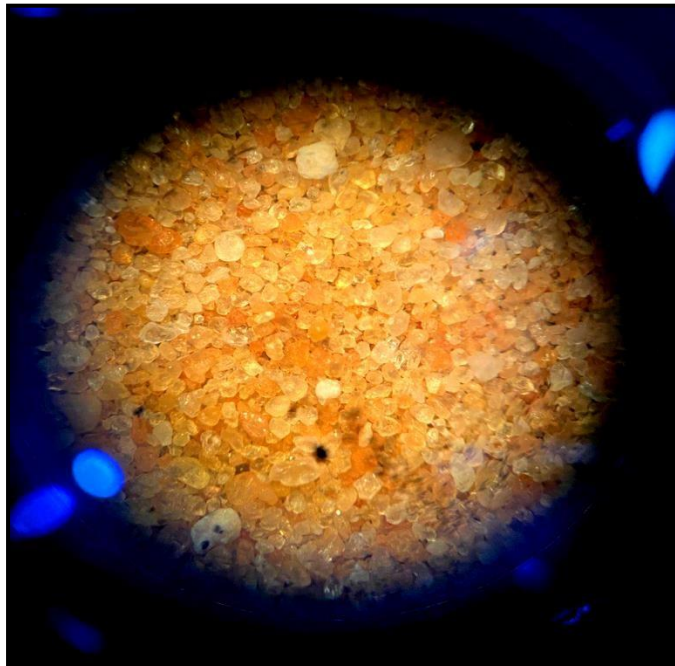
Appendix A

Sand grains of 500 μm diameter under the microscope



Appendix B

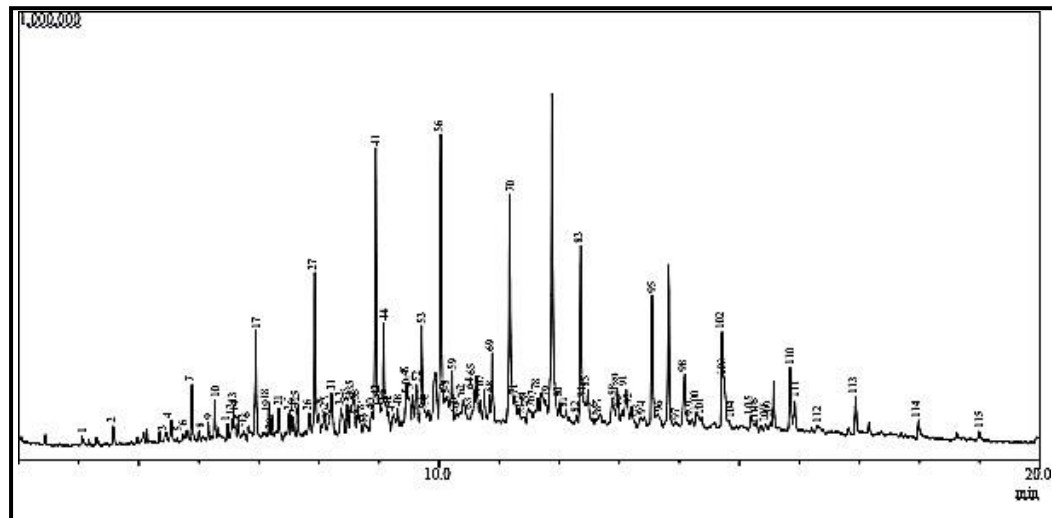
Sand grains of 250 μm diameter under the microscope



Appendix

Appendix C

Diesel chromatographmass spectrometry analysis report



Peak	Area%	Similarity	Index Name
1	0.20	96	767 Heptane, 2-methyl-
2	0.38	93	800 Octane
7	0.92	94	900 Nonane
11	0.32	90	956 1-Octanol, 2-butyl-
12	0.41	95	963 Nonane, 4-methyl-
16	0.30	90	989 Cyclohexane, 1-methyl-2-propyl-
17	2.26	93	1001 Decane
18	0.44	93	1023 Heptane, 3,3,5-trimethyl-
24	0.32	93	1065 Decane, 2-methyl-
27	2.82	97	1101 Undecane
32	1.07	92	1144 Cyclohexane, pentyl-
33	0.68	92	1154 Undecane, 2,5-dimethyl-
35	1.41	93	1164 Dodecane, 2-methyl-
36	0.53	91	1171 Undecane, 3-methyl-
41	5.26	96	1201 Dodecane
44	2.01	94	1213 Undecane, 4,6-dimethyl-
48	0.52	90	1235 Cyclohexane, 2-butyl-1,1,3-trimethyl-
52	1.17	94	1264 Dodecane, 2-methyl-
53	2.46	94	1272 Dodecane, 4,6-dimethyl-
56	6.36	96	1301 Tetradecane

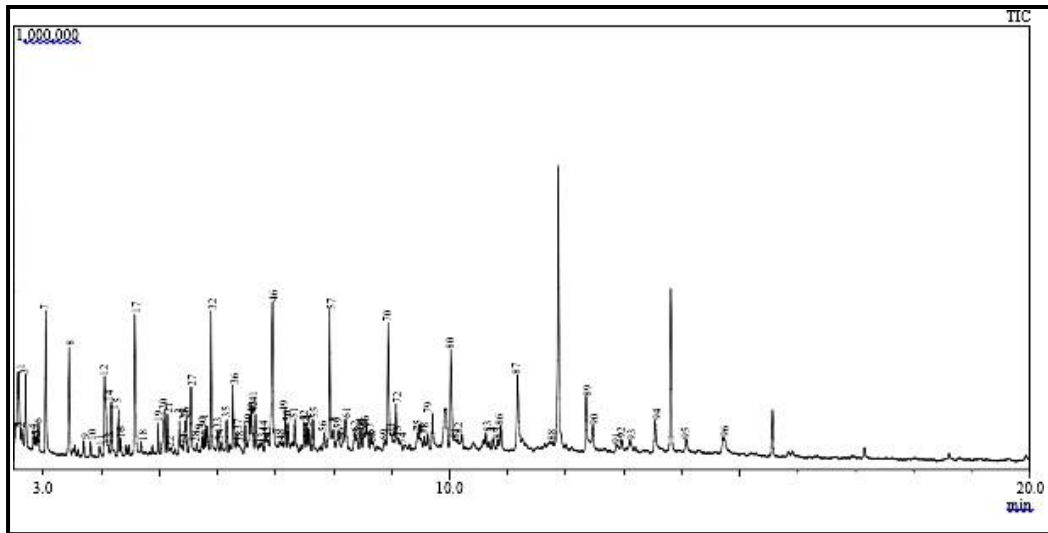
Appendix

67	0.90	92	1364	Heptadecane
69	1.49	92	1376	Dodecane, 2,6,10-trimethyl-
70	5.56	96	1401	Tetradecane
77	0.70	95	1441	Naphthalene, 1,3-dimethyl-
83	3.78	97	1501	Heptadecane
85	1.18	92	1511	Butylated Hydroxytoluene
95	3.21	97	1602	Heptadecane
98	1.64	93	1648	Octadecane
02	2.23	96	1702	Heptadecane
05	0.55	91	1745	Eicosane
10	1.42	96	1803	Heneicosane
11	0.79	92	1810	Eicosane
13	0.87	96	1903	Eicosane
14	0.41	95	2003	Eicosane
15	0.23	92	2104	Eicosane

Appendix

Appendix D

Crude oil chromatographmass spectrometry analysis report



Appendix

Peak	Area%	Similarity	Index Name
1	3.92	90	671 Pentane, 2,4-dimethyl-
2	1.11	93	674 Pentane, 2,3-dimethyl-
3	2.37	96	678 Hexane, 3-methyl-
4	1.20	91	687 Tridecane, 3-methylene-
5	0.52	93	690 Cyclopentane, 1,3-dimethyl-
6	0.80	96	693 Cyclopentane, 1,2-dimethyl-, cis-
7	3.59	96	701 Heptane
8	2.67	98	727 Cyclohexane, methyl-
9	0.39	97	743 Cyclopentane, 1,2,4-trimethyl-
10	0.36	95	751 1,2,3-Trimethylcyclopentane
11	0.34	95	761 Hexane, 2,3-dimethyl-
12	2.79	98	767 Heptane, 2-methyl-
13	0.30	90	770 Hexane, 3,4-dimethyl-
14	1.35	97	774 Heptane, 3-methyl-
15	0.97	96	782 Cyclohexane, 1,3-dimethyl-, cis-
16	0.39	95	785 Cyclohexane, 1,4-dimethyl-
17	3.73	96	800 Octane
18	0.34	96	809 Cyclohexane, 1,4-dimethyl-, cis-
19	0.71	93	831 Octane, 2-methyl-
20	1.49	95	839 Cyclohexane, ethyl-
21	0.86	93	843 Cyclohexane, 1,1,3-trimethyl-
24	0.30	90	862 Heptane, 4-ethyl-
26	0.62	92	868 Octane, 3,4,5,6-tetramethyl-
28	0.44	92	882 Cyclohexane, 1,2,4-trimethyl-
29	0.61	91	889 1-Pentyl-2-propylcyclopentane
30	0.50	95	892 1-Ethyl-3-methylcyclohexane (c,t)
32	3.25	95	900 Nonane
33	0.72	93	912 Cyclohexane, 1-ethyl-2-methyl-
37	0.52	92	942 Octane, 2,3-dimethyl-
40	0.99	95	963 Octane, 2,5-dimethyl-
44	0.67	91	989 Cyclohexane, 1-methyl-2-propyl-
46	4.64	94	1001 Decane

Appendix

62	0.88	92	1144	Cyclohexane, pentyl-
64	0.64	93	1154	Undecane, 2,5-dimethyl-
66	1.16	92	1164	Nonadecane
67	0.38	91	1171	Undecane, 3-methyl-
70	3.38	96	1201	Dodecane
72	1.37	94	1213	Undecane, 4,6-dimethyl-
78	0.45	92	1264	Dodecane, 2-methyl-
79	0.93	93	1272	Dodecane, 4,6-dimethyl-
80	2.91	97	1301	Tetradecane
84	0.39	91	1364	10-Methylnonadecane
85	0.31	90	1371	2-Bromo dodecane
86	0.76	93	1376	Dodecane, 2,6,10-trimethyl-
87	2.60	97	1401	Tetradecane
89	1.98	97	1501	Heptadecane
90	1.00	95	1511	2,6-Di-tert-butyl-4-methyl-phenol
93	0.57	90	1565	Eicosane
94	0.96	96	1602	Heptadecane
95	0.49	93	1648	Heneicosane
96	0.94	96	1702	Heptadecane
